EBioMedicine 51 (2020) 102603

Contents lists available at ScienceDirect

EBioMedicine

journal homepage: www.elsevier.com/locate/ebiom

Research paper

Tumor necrosis factor α-induced protein 1 as a novel tumor suppressor through selective downregulation of CSNK2B blocks nuclear factor-κB activation in hepatocellular carcinoma

Ye Xiao[a,b,d], Shulan Huang[b], Feng Qiu[b], Xiaofeng Ding[a,b], Yi Sun[e], Chenxi Wei[a,b], Xiang Hu[a,b], Ke Wei[f], Shengwen Long[b], Lina Xie[g], Yu Xun[b], Wen Chen[b], Zhijian Zhang[h], Ning Liu[a,b,c,*], Shuanglin Xiang[a,b,*]

[a] State Key Laboratory of Developmental Biology of Freshwater Fish, College of Life Science, Hunan Normal University, Changsha, 410081, China
[b] Key Laboratory of Protein Chemistry and Development Biology of State Education Ministry of China, College of Life Science, Hunan Normal University, Changsha, 410081, China
[c] Key Laboratory of Study and Discovery of Small Targeted Molecules of Hunan Province, School of Medicine, Hunan Normal University, Changsha, 410013, China
[d] Department of Endocrinology, Endocrinology Research Center, Xiangya Hospital of Central South University, Changsha, 410008, China
[e] Department of Pathology, Second Xiangya Hospital of Central South University, Changsha, 410011, China
[f] Medical school, Hunan University of Traditional Chinese Medicine, Changsha, 410208, China
[g] Department of Stomatology, First Affiliated Hospital of Guangzhou University of Chinese Medicine, Guangzhou, 510405, China
[h] Department of Pathology, Xiangya Hospital of Central South University, Changsha, 410008, China

ARTICLE INFO

Article History:
Received 27 August 2019
Revised 10 December 2019
Accepted 10 December 2019
Available online xxx

Keywords:
Tumor necrosis factor α-induced protein 1
Hepatocellular carcinoma
Nuclear factor-κB
Protein kinase casein kinase II beta
Tumor suppressor

ABSTRACT

Background: Tumor necrosis factor α-induced protein 1 (TNFAIP1) is frequently downregulated in cancer cell lines and promotes cancer cell apoptosis. However, its role, clinical significance and molecular mechanisms in hepatocellular carcinoma (HCC) are unknown.

Methods: The expression of TNFAIP1 in HCC tumor tissues and cell lines was measured by Western blot and immunohistochemistry. The effects of TNFAIP1 on HCC proliferation, apoptosis, metastasis, angiogenesis and tumor formation were evaluated by Cell Counting Kit-8 (CCK8), Terminal deoxynucleotidyl transferase dUTP Nick-End Labeling (TUNEL), transwell, tube formation assay *in vitro* and nude mice experiments *in vivo*. The interaction between TNFAIP1 and CSNK2B was validated by liquid chromatography-tandem mass spectrometry (LC-MS/MS), Co-immunoprecipitation and Western blot. The mechanism of how TNFAIP1 regulated nuclear factor-kappaB (NF-κB) pathway was analyzed by dual-luciferase reporter, immunofluorescence, quantitative Real-time polymerase chain reaction (RT-qPCR) and Western blot.

Findings: The TNFAIP1 expression is significantly decreased in HCC tissues and cell lines, and negatively correlated with the increased HCC histological grade. Overexpression of TNFAIP1 inhibits HCC cell proliferation, metastasis, angiogenesis and promotes cancer cell apoptosis both *in vitro* and *in vivo*, whereas the knockdown of TNFAIP1 in HCC cell displays opposite effects. Mechanistically, TNFAIP1 interacts with CSNK2B and promotes its ubiquitin-mediated degradation with Cul3, causing attenuation of CSNK2B-dependent NF-κB trans-activation in HCC cell. Moreover, the enforced expression of CSNK2B counteracts the inhibitory effects of TNFAIP1 on HCC cell proliferation, migration, and angiogenesis *in vitro* and *in vivo*.

Interpretation: Our results support that TNFAIP1 can act as a tumor suppressor of HCC by modulating TNFAIP1/CSNK2B/NF-κB pathway, implying that TNFAIP1 may represent a potential marker and a promising therapeutic target for HCC.

1. Introduction

Hepatocellular carcinoma (HCC) has become the second leading cause of cancer-related deaths worldwide, with an ascending trend in recent years [1]. Frequent intrahepatic and extrahepatic metastasis and active angiogenesis are responsible for the rapid recurrence and

* Corresponding authors.
E-mail addresses: liuning0731@126.com (N. Liu), xshlin@hunnu.edu.cn (S. Xiang).

https://doi.org/10.1016/j.ebiom.2019.102603

Research in context

Evidence before this study

Hepatocellular carcinoma (HCC), accounts for approximately 90% of primary liver cancers, has become one of the most notable lethal malignancies worldwide. Frequent intrahepatic and extrahepatic metastasis and active angiogenesis is a serious problem in the management of HCC. Tumor necrosis factor α-induced protein 1 (TNFAIP1) was initially identified as a TNFα and LPS induced gene and has been correlated with some cancer cell apoptosis and migration. However, whether TNFAIP1 protein regulates metastasis and angiogenesis in HCC remains mostly unknown, necessitating further exploration.

Added value of this study

In this study, we have reported some novel biological roles of TNFAIP1, a novel tumor suppressor, in hepatocellular carcinoma. TNFAIP1 suppresses HCC cell proliferation, metastasis, angiogenesis and promoted apoptosis *in vitro* and *in vivo* through selective down-regulation of CSNK2B blocks CSNK2B-dependent NF-κB pathway.

Implications of all the available evidence

Our findings identify a novel signaling pathway in TNFAIP1-regulated inhibition of HCC cell metastasis, angiogenesis, and tumorigenesis, which may represent a new marker and a promising therapeutic target for HCC therapy.

poor survival of HCC [2]. So far, the molecular mechanisms underlying HCC metastasis and angiogenesis are still largely unknown. Hence, elucidation of mechanism-related biomolecules underlying the metastasis and angiogenesis in HCC and the identification of novel therapeutic targets are crucial.

Tumor necrosis factor α-induced protein 1 (TNFAIP1), also known as B12 or BACURD2, was initially identified as a tumor necrosis factor alpha (TNFα)- and lipopolysaccharide (LPS)-induced gene in umbilical vein endothelial cells [3]. In mammals, the amino acid sequences of TNFAIP1 are highly similar to polymerase delta-interacting protein 1 (PDIP1) and potassium channel tetramerization domain containing 10 (KCTD10), where all of them contain a conserved BR-C, ttk, and bab (BTB)/Pox virus and zinc finger (POZ) domain and a proliferating cell nuclear antigen (PCNA) binding motif [4]. Abundant evidence indicates that TNFAIP1 is implicated in many cellular processes, including cell movement and migration [5–8], apoptosis [9], and immune response [10]. Aberrant expression of TNFAIP1 has been reported to be associated with multiple diseases including hepatitis B virus (HBV) infection, neuropathic pain, and Alzheimer's disease (AD) [10–12]. Importantly, emerging evidence suggests that TNFAIP1 is critically involved in cancer metastasis and progression in non-small cell lung cancers (NSCLCs) [6,7], uterine cancer [13], gastric carcinoma [14], etc. However, the role and the underlying mechanisms of TNFAIP1 in HCC have been rarely reported.

Nuclear factor kappa-light-chain-enhancer of activated B cells (NF-κB) is a dimeric transcription factor that plays a vital role in cell proliferation, apoptosis, metastasis, and angiogenesis [15]. NF-κB dimers are formed by the association of two of the following monomers: P65 (RelA), p50 (NF-κB1), p52 (NF-κB2), RelB, and c-Rel. In most types of cells, NF-κB dimers are inactive in the cytoplasm, and only control gene expression when activated and translocated into the nucleus [15]. There are three NF-κB-activating pathways. The first pathway, also called the classical pathway, is dependent on the activation of the IκB-kinase (IKK) complex (IKKα, IKKβ, and IKKγ). Once the IKK complex is activated, it mediates IκB phosphorylation and then induces IκB ubiquitination and degradation, which leads to the release and translocation of NF-κB heterodimer, p65/p50, into the nucleus and activates gene expression. The second pathway, also named the alternative pathway, involves NF-κB-inducing kinase (NIK), which mediates the activation of IKKα homodimer and then processes p100/RelB into the p52/RelB heterodimer, and subsequently triggers the nuclear translocation of p52/RelB. The third pathway is named the atypical pathway, and is activated by casein kinase 2 (CK2) and also requires the degradation of IκBs [16]. Accumulating evidence indicates that CK2 promotes aberrant NF-κB activation by phosphorylating IKK and IκBs, enhancing IκB proteasomal degradation, and also directly phosphorylating p65 to finally increase NF-κB transcriptional activity [17–19]. Previously, we found that TNFAIP1 can bind CSNK2B (CK2β, a regulatory subunit of CK2) and can be phosphorylated by CK2 [20]. We also found that overexpression of TNFAIP1 suppresses NF-κB activation in Hek293FT cells [21]. However, it is unclear how TNFAIP1 suppresses NF-κB activation and whether TNFAIP1-mediated suppression of NF-κB activation is associated with CSNK2B in HCC.

In this study, we show that TNFAIP1 acts as a negative regulator of HCC proliferation, apoptosis, metastasis, and angiogenesis by blocking the TNFAIP1/CSNK2B/NF-κB pathway. Our results indicate that TNFAIP1 might represent a potential therapeutic target for HCC.

2. Materials and methods

2.1. Patient tissue specimens

A series of 80 hepatocellular carcinoma tumor tissues and corresponding peritumor tissues were collected from the Second Xiangya Hospital of Central South University. A series of 20 hepatocellular carcinomas with lymph nodes metastasis tissues were collected from the Second Xiangya Hospital of Central South University. This study was approved by the Ethics Committee of Hunan Normal University and the second Xiangya Hospital of Central South University. All of the patients signed informed consent.

2.2. Mice

BALB/c female nude mice (4 weeks old) were purchased from Hunan Slaccas Jingda (Changsha, China). All mice were housed in the specific pathogen-free facility of the Laboratory Animal Research Center with 12 h light /12 h dark cycles and adequate water and food. All animal care protocols and experiments were reviewed and approved by the Ethics Committee of Hunan Normal University.

2.3. Cell culture, plasmid construction

Human hepatocellular carcinoma cell lines including HepG2, Bel-7402, Hep3B, SMMC7721 and MHCC97H and hepatocyte line LO2, and human umbilical vascular endothelial cells (HUVEC) were purchased from the Chinese Academy of Sciences Shanghai Branch Cell Bank (Shanghai, China). All cell lines were cultured in Dulbecco's modified Eagle medium (DMEM, Gibco) contained 10% fetal bovine serum (FBS, Gibco) and 1% penicillin/streptoMycin at 37 °C in a 5% CO_2 incubator.

The Myc-tagged TNFAIP1 expression vector was constructed as we previously described [21]. The HA-tagged CSNK2B expression vector was constructed by inserting full-length CSNK2B coding sequence into pCMV-HA vector. Meanwhile, N-terminus (the BTB domain), C-terminus and the full-length CDS region of TNFAIP1 were also cloned into pGEX-4T-2 vector, meanwhile, the full-length CDS region of CSNK2B was inserted pET-32a (+) vector. The primers for vectors construction were described in Supplementary Table S1. His-Cul3, Rbx1 and His-ubiquitin plasmids were purchased from Sino

Biological Inc (China). Reporter plasmid NF-κB-Luc was kindly provided by dr. Xiang Hu (Hunan Normal University).

2.4. Generation of stable cell lines

The lentiviral particles overexpressing TNFAIP1, CSNK2B and coding shRNAs against TNFAIP1, Cul3 and CSNK2B were purchased from Hanbio Biotechnology (Shanghai, China). The empty vector was used as a control. MHCC97H cells were infected with Control and TNFAIP1 lentiviral particles with a multiplicity of infection (MOI) of 50 to 100 and then selected with 4 μg/ml puroMycin (Gibco) to generate MHCC97H—Control and MHCC97H-TNFAIP1 stable cell lines, respectively. SMMC7721 cells were infected with shControl and shTNFAIP1 lentiviral particles to generate SMMC7721-shControl and SMMC7721-shTNFAIP1 stable cell lines, respectively. HUVECs were infected with Control lentiviral, TNFAIP1 lentiviral, shControl lentiviral, and shTNFAIP1 lentiviral particles to generate HUVEC—Control, HUVEC-TNFAIP1, HUVEC-shControl and HUVEC-shTNFAIP1 stable cell lines. The selected stable cells were used for experiments. The target sequences for shTNFAIP1 were as follows: shTNFAIP1-1, 5′- TGGGCAACAAGTATGTCCAGCTCAA; shTNFAIP1-2, 5′- CGTGCTCTTCATCAAGGATGT-3′; shTNFAIP1-3 5′- GCAACAAGTATGTCCAGCTCA −3′. The target sequences for shCul3 were as follows: shCul3-1 5′-TTGACGTGAACTGACATCCACATTC-3′; shCul3-2 5′-TACATATGTGTATACTTTGCGATCC-3′. The target sequences for shCSNK2B were as follows: 5′-TGGTTTCCCTCACATGCTCT-3′.

2.5. RNA isolation and quantitative real-time polymerase chain reaction (RT-qPCR)

Total RNA was extracted from cultured cells or tissues using Trizol Reagent (Invitrogen, USA). Purified RNA (1 μg) was reversely transcribed into cDNA with PrimeScript™ RT reagent Kit with gDNA Eraser (Takara, Japan) after determining the concentration by Nanodrop2000 (Thermofisher, USA). RT-qPCR was analyzed with the SYBR PrimeScript RT-qPCR Kit (Takara, Japan) for 40 cycles at 95 °C for 5 s, 60 °C for 30 s in 7900HT Fast RT-qPCR System (Applied Biosystems). The primers of TNFAIP1, RhoB, Bcl2, Bcl-XL, CCND1, MMP2, MMP9, VEGF and β-actin were shown in Supplementary Table S1. The relative transcript levels of the target gene were given by $2^{-\triangle\triangle Ct}$ method using β-actin as an internal control.

2.6. Western blot analysis

Tissues and treated cells were harvested and lysed in RIPA buffer containing a protease inhibitor cocktail (1:100). Total protein was extracted and the concentration was determined by the BCA method (Thermofisher, USA). And then equal amounts of total protein were separated by 12% SDS-PAGE and transferred onto polyvinylidene difluoride (PVDF) membranes (Millipore, USA). The membranes were blocked, washed (4 × 10 min), and incubated with the primary antibodies which were shown in Supplementary Table S2. Protein bands were washed (4 × 10 min) and then incubated with secondary anti-mouse or anti-rabbit peroxidase-linked antibodies (KPL, USA). Protein bands were then washed (4 × 10 min) and visualized using an enhanced chemiluminescence assay kit (SuperSignal PierceBiotechnology, USA). Three replicates were performed for all Western blot analysis.

2.7. Immunohistochemistry and scoring

Liver and xenograft tissues were fixed by 4% paraformaldehyde, then, paraffin-embedded for immunohistochemical study as previously described [22]. The primary antibodies used in immunohistochemistry were shown in Supplementary Table S2. The stained tumors were quantified using a scoring system from 0 to 10, in which a score greater than 3 was defined as high expression and a score less than 3 as low expression. The score was calculated by multiplying the intensity of signals with the percentage of positive cells. The signal intensity was scored as no signal (0), weak signal (1), moderate signal (2), and strong signal (3). The percentage of positive cells was also scored as 0% (0), 1−25% (1), 25−50% (2), and ≥50% (3) [22,23].

2.8. Immunofluorescence

MHCC97H—Control, MHCC97H-TNFAIP1, SMMC7721-shControl and SMMC7721-shTNFAIP1 stable cell lines were seeded into 24-well culture plate with glass covers. After 48 h, cells were fixed with 4% formaldehyde and subjected to permeabilization with 0.2% Triton X-100. The cells blocked with 1% BSA and incubated with the indicated antibodies which were shown in Supplementary Table S2, followed by marking nuclei with DAPI (Beyotime Biotechnology, China). Images were captured using Diaphot Inverted Microscope Camera System (Leica) [24].

2.9. Co-Immunoprecipitation (Co-IP) assay

Co-Immunoprecipitation assay was performed as previously described [8]. Briefly, cells were collected and lysed in 1% NP-40 buffer (250 mM NaCl, 1% NP-40, 50 mM HEPES, 5 mM EDTA) at 48 h post-transfection. Lysates were centrifuged for 10 min at 14,000 g, and the supernatant was precleared with Protein A/G beads (Santa Cruz). After centrifugation, the precleared supernatant was incubated with indicated antibodies against TNFAIP1, CSNK2B, Myc, HA (shown in Supplementary Table S2) and pre-immune mouse IgG (Cell Signaling Technology) served as negative control overnight at 4 °C. The following day, protein complexes were added with 50 μl of Protein A/G beads and incubated for 3 h at room temperature. The collected protein complexes were washed 5 times with RIPA buffer and separated by 12% SDS-PAGE, and then analyzed by immunoblotting with TNFAIP1, CSNK2B, Myc and HA antibody.

2.10. LC-MS/MS assay

For liquid chromatography-tandem mass spectrometry (LC-MS/MS) analysis, MHCC97H cells transfected with Myc-tagged TNFAIP1 plasmid and subjected to incubation with anti-Myc antibody. The potential TNFAIP1-binding proteins were pulled down by Co-IP and performed with LC-MS/MS analysis. Briefly, the proteins solution, pulled down by Co-IP, was separated by 12% SDS-PAGE. After electrophoresis, the protein gel was sliced and washed with acetonitrile (ACN) and followed by natural drying. The drying protein gel pieces were reduced with 10 mM DTT for 40 min at 56 °C and subsequently alkylated with 50 mM IAM for 30 min in the dark. And then the protein gel pieces were digested with trypsin (Gibco) overnight at 37 °C. After digestion, the peptides were extracted with 0.1% formic acid (FA) and desalted with C18 cartridge and dried by vacuum centrifugation. The Orbitrap Q Exactive HF-X mass spectrometer (Thermo Fisher) and EASY-nLCTM 1200 UHPLC system (Thermo Fisher) was used to identify the peptides according to the standard protocols [25]. The raw and msfsearch document of LC-MS/MS analysis for identifying TNFAIP1-interaction proteins have been uploaded to ProteomeXchange (ID: PXD016378).

2.11. Protein purification and GST pull-down assay

GST-TNFAIP1(1−316), GST-TNFAIP1-N terminal (1−96), GST-TNFAIP1-C terminal (97−316), GST and His-CSNK2B fusion proteins were expressed in BL21 (DE3) Escherichia coli cells, induced by 0.1 mM isopropyl-β-D-thiogalactoside (IPTG) at 37 °C for 3 h. Purification of GST fusion proteins and His-fusion proteins were performed as previously described [26]. For GST pull-down assay, equal amounts (5 μg) of GST and GST-fused indicated regions of TNFAIP1 protein

were incubated with 50 μl glutathione-Sepharose 4B beads. The coated beads were then incubated with purified His-CSNK2B protein (5 μg) for 2 h at 4 °C. After being washed with PBS, the sample was denatured and analyzed by immunoblotting with indicated antibodies (Supplementary Table S2).

2.12. Ubiquitination assay

MHCC97H cells were infected with shTNFAIP1 and shControl lentiviral particles or HEK293FT was transfected with His-ubiquitin, His-Cul3, HA-CSNK2B, Rbx1 and Myc-TNFAIP1 plasmid for 48 h, and then treated with 25 mM MG132 for 4 h. Cells were harvested and lysed in 1% NP-40 buffer for 30 min on ice. The lysates were centrifuged and the supernatants were incubated with HA antibody (Cell Signaling Technology) overnight at 4 °C. The following day, protein complexes were added with 50 μl of Protein A/G beads and incubated for 3 h at room temperature. The immunoprecipitates were washed five times with PBS, denatured and analyzed by immunoblotting with ubiquitin antibody (Cell Signaling Technology) and other indicated antibodies (Supplementary Table S2).

2.13. Cell proliferation and TUNEL assays

MHCC97H-TNFAIP1, MHCC97H—Control, SMMC7221-shTNFAIP1 and SMMC7221-shControl stable cell lines were seeded into 96-well culture plate and incubated with CCK8 solution (1:100, MCE, China) for 4 h. MHCC97H and SMMC7721 were infected with TNFAIP1, TNFAIP1/CSNK2B or Control lentiviral particles to generate MHCC97H-TNFAIP1, MHCC97H-TNFAIP1-CSNK2B, SMMC7721-TNFAIP1, SMMC7721-TNFAIP1-CSNK2B and Control stable cells, and were seeded into 96-well culture plate for 48 h, and then incubated with CCK8 solution (1:100, MCE, China) for 4 h. The absorption of the culture medium was measured using a multi-wavelength measurement system (Thermo Fisher, USA) at 490 nm. Cell apoptosis assay was performed using the Dead End Fluorometric TUNEL System (Roche, Germany), as previously described [27].

2.14. Transwell migration and invasion assays

The migration assays were conducted using an 8 μm transwell apparatus (Merckmillipore, USA) as described [28]. For cell invasion assay was determined by using an 8 μm BD Matrigel-coated invasion chamber (BD Bioscience, USA). Cells in serum-free medium (200 μl, 2×10^4 cells) were added to the upper chamber, while culture medium (600 μl) was placed in the lower chamber. Eighteen hours later, filters were fixed with 4% formaldehyde and stained with 0.4% crystal. Migrated and invaded cells on the underside of the filters were photographed and counted in five random fields of each filter.

2.15. Tube formation assay

The tube formation assay was performed by keeping 24-well culture plates on ice and coated with 200 μl of chilled Corning Matrigel Matrix (BD Biosciences, USA) per well. Incubate plates at 37 °C for 30 min, where it would polymerize. A volume of 200 μl of 1.2×10^5 cells of HUVEC—Control, HUVEC-TNFAIP1, HUVEC-shControl, HUVEC-shTNFAIP1 stable cells were seeded onto matrigel-coated plates. After 16 h, tubules were captured using Diaphot Inverted Microscope Camera System (Leica) and the length and the number of branch points was quantified for using NIH Image J software.

2.16. Lung metastasis assays

In vivo lung metastasis assays were estimated by tail vein injection, MHCC97H-TNFAIP1 stable cells (2×10^6) or SMMC7721-shTNFAIP1 stable cells (2×10^6) and control stable cells were injected into 4-week-old female nude mice ($n = 7$ mice/group) tail vein, respectively. After 6 weeks, the mice were sacrificed and the lungs were excised, the occurrence of lung metastasis was counted and analyzed by Hematoxylin and Eosin (HE) staining [29].

2.17. In vivo *functional assay*

The MHCC97H-TNFAIP1 stable cells (0.5×10^7) and SMMC7721-shTNFAIP1 stable cells (0.5×10^7) were injected subcutaneously into the back of 4-week-old BALB/c female nude mice ($n = 5$ mice/group, Hunan Slaccas Jingda, China), respectively. The control group was injected with SMMC7721-shcontrol stable cells or MHCC97H-control stable cells. The length and width of the tumors were measured weekly with a vernier caliper. Primary tumor volume was calculated with the formula: volume = width^2 × length/2. After 6 weeks, the nude mice were sacrificed and tumors were measured, photographed and weighed. All mouse experiments were approved by Hunan Normal University Animal Care and Use Committee.

2.18. Statistical analysis

Statistical analyses were performed with SPSS 13.0 (SPSS, Inc., Chicago, IL, USA). Data are shown as means ± SEM. The association between TNFAIP1 expression and HCC patients' clinicopathological variables were analyzed using Pearson's $\chi 2$ test. For comparisons of 2 groups, a 2-tailed Student's *t*-test was used. Comparisons of multiple groups were performed by using one-way analysis of variance (ANOVA) followed by Dunnett's post hoc test. All experiments were repeated at least 3 times. Statistical significance was concluded at $^*P < 0.05$, $^{**}P < 0.01$, $^{***}P < 0.001$.

3. Results

3.1. TNFAIP1 expression is reduced in HCC tissues and cell lines

To detect the level of TNFAIP1 in HCC, we collected 80 pairs of HCC tumor tissues and peritumor tissues from the Second Xiangya Hospital of Central South University. Western blot analysis showed that TNFAIP1 protein levels in HCC tumor tissues were remarkably lower than that in paired peritumor tissues (Fig. 1a and b). This observation was further confirmed by immunohistochemical (IHC) staining with the anti-TNFAIP1 antibody. Consistently, the intensity of positively stained tumor tissues and the staining score of TNFAIP1 were decreased gradually along with the increased tumor histological grade (I, II, and III) (Fig. 1c and e); and staining score analysis also displayed that TNFAIP1 expression was significantly lower in HCC tissues than that in peritumor tissues (Fig. 1d). Moreover, TNFAIP1 expression was negatively correlated with the histological grade of HCC (Pearson's correlation coefficient, −0.6129, $P < 0.0001$, Fig. 1f). Furthermore, we also found that TNFAIP1 expression was significantly lower in hepatocellular carcinoma with lymph nodes metastasis tissues (Supplementary Figure1). Clinicopathological association analyses of the 80 HCCs revealed that TNFAIP1 expression was significantly associated with tumor size (Pearson's $\chi 2$ test, $P < 0.05$), tumor stage (Pearson's $\chi 2$ test, $P < 0.05$) and tumor differentiation (Pearson's $\chi 2$ test, $P<0.01$) (Table 1). Next, the expression of TNFAIP1 in HCC cell lines was detected. The results showed that the HCC cell lines, including HepG2, Bel-7402, Hep3B, SMMC7721, and MHCC97H, displayed significantly lower mRNA and protein levels than normal liver cells LO2 (Fig. 1g and h). These results suggest that TNFAIP1 expression is decreased in HCC tissues and cell lines.

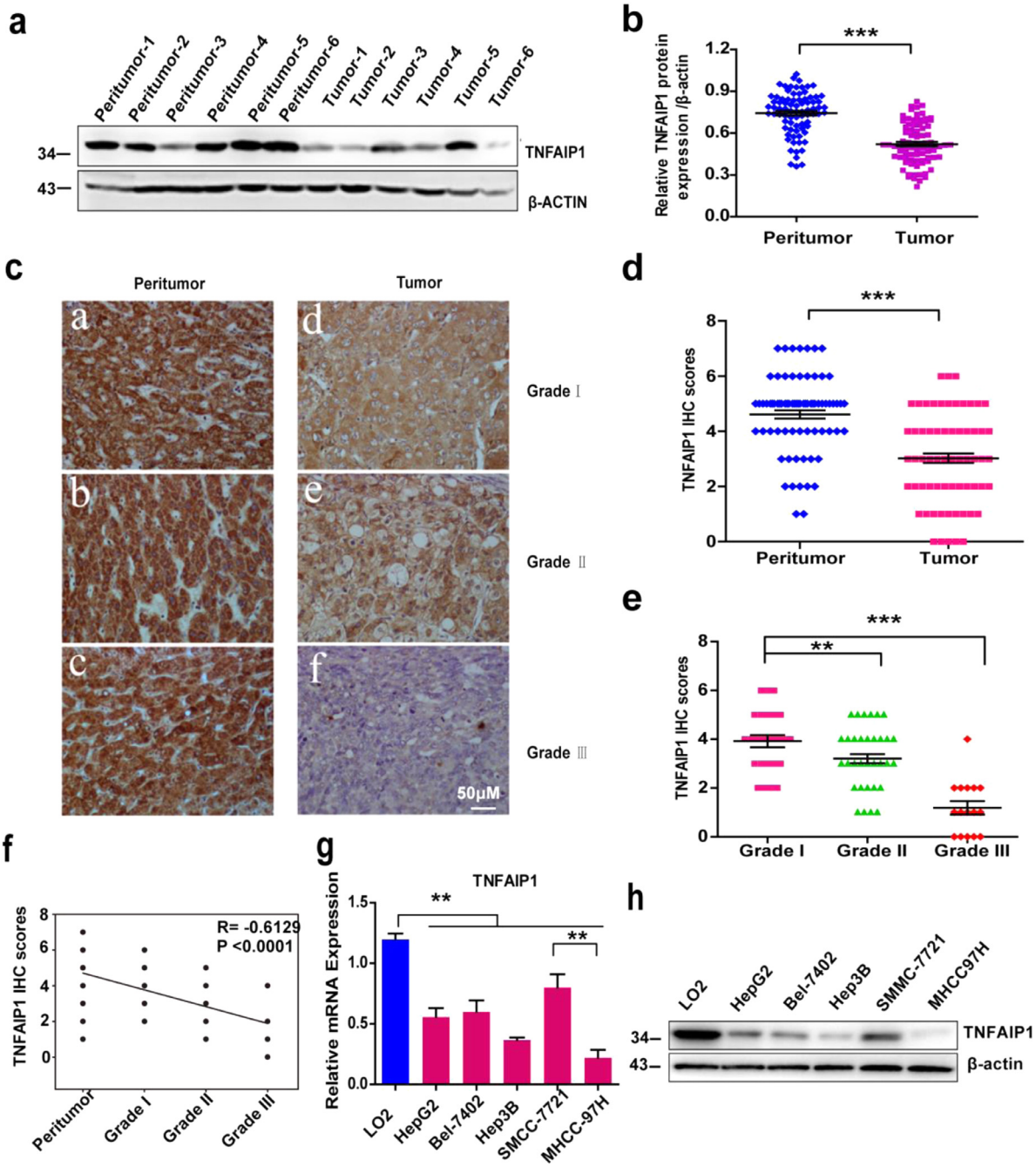

Fig. 1. TNFAIP1 is low-expressed in human HCC specimens and cell lines. a. Western blot analysis of TNFAIP1 protein expression in HCC peritumor tissues and tumor tissues, β-actin was used as a loading control. b. The protein expression of TNFAIP1 (normalized according to the expression of β-actin) in peritumor tissues and tumor tissues was quantified (***P<0.001, Student's t-test). c. Representative photograph of TNFAIP1 protein expression in peritumor and HCC tumor tissues. Scale bar, 50 μm. d. Quantitative analysis of the staining score of TNFAIP1 in peritumor tissues and HCC tumor tissues (***P < 0.001, Student's t-test). e. Quantitative analysis of the staining score of TNFAIP1 in different tumor grades of human HCC (**P < 0.01, ***P < 0.001, Student's t-test). f. SigmaPlot software was used to analyze the correlation between the staining score of TNFAIP1 and HCC grade (Pearson's correlation coefficient, −0.6129, ***P<0.0001). g. RT-qPCR was used to analyze the mRNA level of TNFAIP1 in a normal hepatocyte cell line (LO2) and human HCC cell lines (HepG2, Bel7402, Hep3B, SMMC7721 and MHCC97H) (**P < 0.01, one-way ANOVA). h. Western blot analysis of TNFAIP1 protein expression in a normal hepatocyte cell line (LO2) and five human HCC cell lines (HepG2, Bel7402, Hep3B, SMMC7721 and MHCC97H). β-actin was used as a loading control. Data are presented as means ± SEM. P-values were determined by two-tailed Student's t-test or one-way ANOVA (**P < 0.01, ***P < 0.001).

3.2. TNFAIP1 inhibits HCC cell proliferation and tumorigenicity, and induces HCC cell apoptosis

The expression of TNFAIP1 is significantly lower in HCC tissues and cells, implying that TNFAIP1 may negatively regulate HCC cell proliferation and tumorigenicity. To investigate the role of TNFAIP1 in HCC cell, lentivirus-mediated TNFAIP1 overexpression and a short hairpin RNA (TNFAIP1-shRNA) vector were respectively introduced into highly invasive MHCC97H cells and less invasive SMMC7721 cells, to generate MHCC97H—Control, MHCC97H-TNFAIP1, SMMC7721-shControl and SMMC7721-shTNFAIP1 stable cell lines. RT-qPCR and Western blot assay confirmed that TNFAIP1 was overexpressed in MHCC97H cells (Fig. 2a and b) and was knocked down in SMMC7721 cells (Fig. 2a and b). Next, Cell Counting Kit-8 (CCK8) assay was performed to test the effect of TNFAIP1 on HCC cell proliferation. The results indicated that overexpression of TNFAIP1

Table 1
Analysis of correlation between TNFAIP1 expression and clinicopathological factors in HCC.

Characteristics	TNFAIP1 Expression (%)			p value
	High (n = 33)	Low (n = 47)	Total	
Age (years)				0.353
≤49	14	23	37	
>49	19	24	43	
Gender				0.236
Male	28	40	68	
Female	5	7	12	
Tumor size (cm)				
≤5	8	16	24	0.037
>5	25	31	56	
Tumor stage				
I/II	27	26	53	0.014
III	6	21	27	
Differentiation				
Well	24	30	54	0.008
poor	9	17	26	

inhibited proliferation in MHCC97H cells (Fig. 2c), and the knockdown of TNFAIP1 increased proliferation in SMMC7721 cells (Fig. 2c). To investigate the effect of TNFAIP1 on tumor growth, we constructed a xenograft tumor mouse model by subcutaneous injection of MHCC97H-TNFAIP1 and SMMC7721-shTNFAIP1 stable cells, infected with lentivirus expressing TNFAIP1 or shTNFAIP1-3 (with best interference effect, Fig. 2a), respectively, into nude mice (n = 5 mice/group). The results showed that the growth rate and the average weights of the tumors derived from MHCC97H-TNFAIP1 stable cells were significantly slower and lighter than tumors derived from control cells (Fig. 2d and e). Conversely, the knockdown of TNFAIP1 in SMMC7721-shTNFAIP1 stable cells significantly accelerated the growth of xenograft tumors and increased tumor weight (Fig. 2f and g) compared with the control cells. To further verify the role of TNFAIP1 in proliferation, xenograft tumors induced by MHCC97H-TNFAIP1 stable cells or SMMC7721-shTNFAIP1 stable cells were stained with Ki67 IHC staining. The results confirmed that the TNFAIP1 overexpression markedly decreased the expression of the proliferation marker, Ki67, in MHCC97H-TNFAIP1-derived xenografts compared to the control tissues (Fig. 2h and i); whereas, the knockdown of TNFAIP1 resulted in upregulation of Ki67 in SMMC7721-shTNFAIP1-derived xenografts compared to the control tissues (Fig. 2h and i). These results indicate that TNFAIP1 inhibits proliferation and the tumorigenic ability of HCC cell.

Previous studies indicate that TNFAIP1 plays an important role in cell apoptosis [9,14,30]. In this study, we found that the overexpression of TNFAIP1 promoted apoptosis in MHCC97H-TNFAIP1 stable cells compared with the control cells by TUNEL assay (Fig. 2j and k). Conversely, the opposite results were found in SMMC7721-shTNFAIP1 stable cells (Fig. 2j and k). Subsequently, RT-qPCR and Western blot assay were used to detect apoptosis-related genes and proteins in both SMMC7721 and MHCC97H stable cells. Not surprisingly, MHCC97H-TNFAIP1 stable cells showed increased levels of Cleaved-caspase3, but decreased levels of anti-apoptotic Bcl-XL and Bcl-2, in comparison to the control cells (Fig. 2l and m). Whereas, the knockdown of TNFAIP1 markedly decreased Cleaved-caspase3 levels, but increased Bcl-XL and Bcl-2 levels in SMMC7721-shTNFAIP1 stable cells, compared to the control cells (Fig. 2l and m). However, the expression of Bax was not changed in MHCC97H-TNFAIP1 stable cells or in SMMC7721-shTNFAIP1 stable cells compared with the control cells (Fig. 2l and m). These data indicate that TNFAIP1 is a potent inducer of apoptosis in HCC cell, and that this apoptosis involves the caspase-related pathway. Interestingly, we also found that TNFAIP1 markedly increased the mRNA and protein expression levels of RhoB (Fig. 2l and m), which has been reported to promote apoptosis of HeLa cells via interaction with TNFAIP1 [9], implying that RhoB may also be involved in TNFAIP1-induced apoptosis of HCC cell.

3.3. *TNFAIP1 inhibits HCC cell migration, invasion, and metastasis* in vitro *and* in vivo

To further examine whether TNFAIP1 suppresses migration and invasion of HCC cell, a transwell assay was performed. The results showed that the number of migrated and invaded cells in the MHCC97H-TNFAIP1 group was significantly lower than that in the control group (Fig. 3a and b); whereas, the number of migrated and invaded cells in the SMMC7721-shTNFAIP1 group was significantly increased compared with the control group (Fig. 3c and d), indicating that TNFAIP1 inhibits HCC cell migration and invasion. To further investigate the role of TNFAIP1 in regulating migration and invasion of HCC cell *in vivo*, MHCC97H-TNFAIP1 and SMMC7721-shTNFAIP1 stable cell lines were respectively intravenously injected into 4-week-old female nude mice through the tail vein. Six weeks after injection, all the mice were sacrificed and their lungs were removed. The number of metastatic nodules on the surface of mouse lungs was counted and lung sections were stained using a hematoxylin and eosin (HE) staining kit. Lung metastatic nodules were fewer and smaller in MHCC97H-TNFAIP1-derived lung tissues than that in the control group (Fig. 3e and f); however, mice injected with SMMC7221-shTNFAIP1 stable cells showed a higher number and larger lung metastatic nodule than the control group (Fig. 3g and h). The expression of TNFAIP1 in lungs of nude mice was confirmed by RT-qPCR. The result showed that TNFAIP1 was overexpressed in MHCC97H-TNFAIP1-derived nude mice and was knocked down in SMMC7721-shTNFAIP1-derived nude mice (Fig. 3i). All nude mice livers had no obvious morphological changes (the data are not shown). Taken together, these findings indicate that TNFAIP1 inhibits HCC cell migration, invasion, and metastasis *in vitro* and *in vivo*.

Because the ability of cell proliferation and invasion is closely associated with the expression of cyclin D1 (CCND1) and matrix metalloproteinases (MMPs), we then examined the expression levels of CCND1, MMP2, and MMP9 in MHCC97H-TNFAIP1 stable cells and SMMC7221-shTNFAIP1 stable cells, respectively. Compared with the vector control, the mRNA and protein levels of CCND1, MMP2, and MMP9 were significantly decreased in MHCC97H-TNFAIP1 stable cells, but were increased in SMMC7221-shTNFAIP1 stable cells (Fig. 3j and k). To further confirm the results, xenograft tumors induced by MHCC97H-TNFAIP1 stable cells or SMMC7721-shTNFAIP1 stable cells were stained with CCND1, MMP2, MMP9, and TNFAIP1 antibodies. The results showed that there were markedly lower levels of CCND1, MMP2, and MMP9 in MHCC97H-TNFAIP1-derived xenografts than the control tissues (Fig. 3l). However, much higher levels of CCND1, MMP2, and MMP9 were found in SMMC7721-shTNFAIP1-derived xenografts than in the control tissues (Fig. 3l). Similar results were observed by western blot analysis (Fig. 3m). These results indicate that TNFAIP1 inhibits HCC cell proliferation, migration, and invasion through downregulation of CCND1, MMP2, and MMP9.

3.4. *TNFAIP1 inhibits HCC angiogenesis and decreases vascular endothelial growth factor (VEGF) expression* in vitro *and* in vivo

To investigate whether TNFAIP1 was involved in HCC-induced angiogenesis, xenograft tumors induced by MHCC97H-TNFAIP1 stable cells or SMMC7721-shTNFAIP1 stable cells were IHC stained with CD31 antibody. The results demonstrated that significantly lower blood vessel density was observed in MHCC97H-TNFAIP1-derived xenografts than the control tissues (Fig. 4a). In addition, the knockdown of TNFAIP1 significantly increased the blood vessel density in SMMC7721-shTNFAIP1-derived xenografts compared with the control tissues (Fig. 4b). To further verify the role of TNFAIP1 in tumor angiogenesis, tube formation was conducted with HUVECs cells.

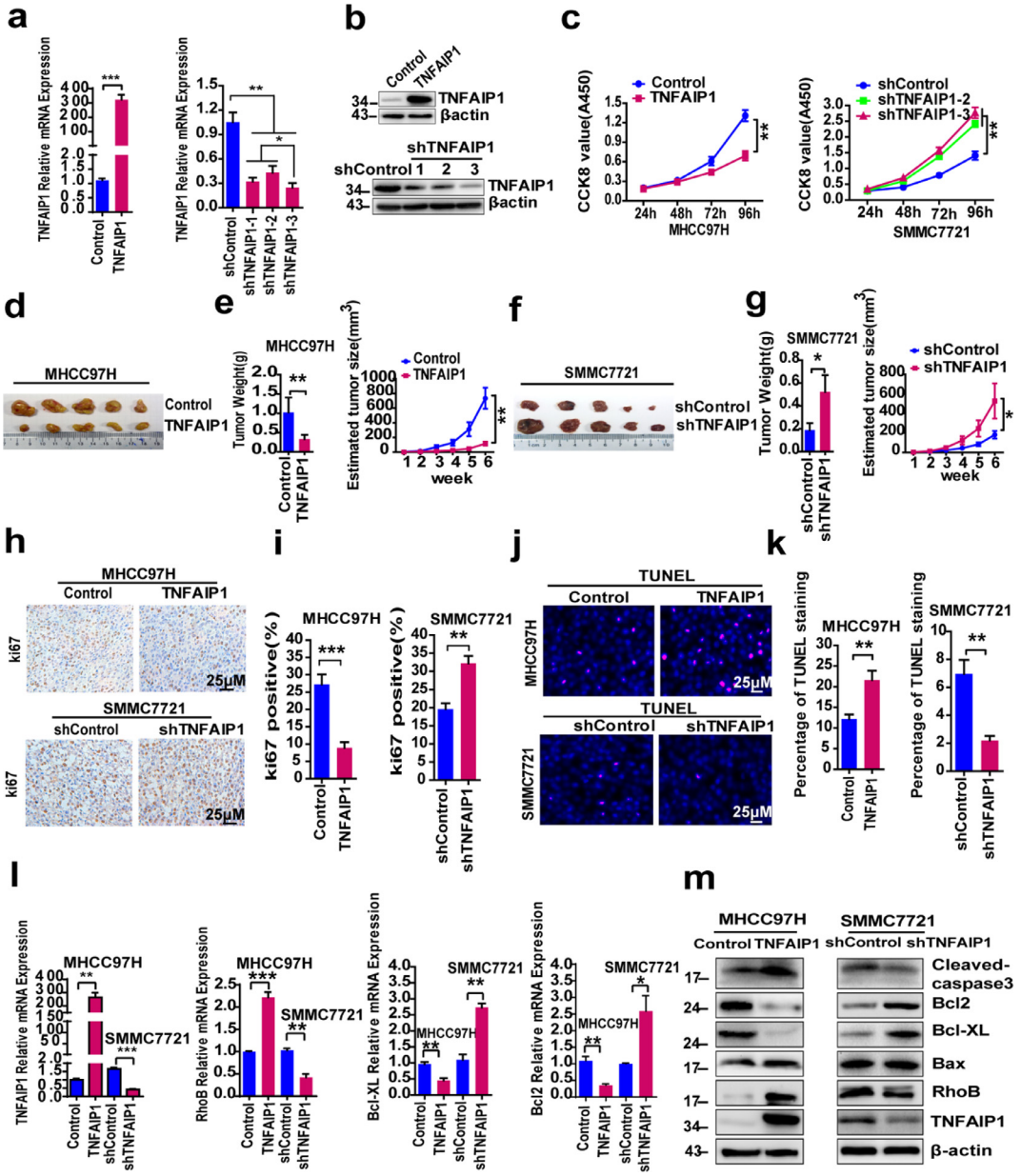

Fig. 2. The effect of TNFAIP1 on HCC cell proliferation, apoptosis and tumor growth. a. RT-qPCR analysis of the mRNA level of TNFAIP1 in MHCC97H cells infected with TNFAIP1 or the control lentivirus (left) (***P<0.001, Student's t-test) and in SMMC7721 cells infected with shTNFAIP1 or shControl lentivirus (right) (*P < 0.05, **P < 0.01, one-way ANOVA). b. Western blot analysis of TNFAIP1 protein expression in MHCC97H infected with TNFAIP1 or the control lentivirus (upper) and in SMMC7721 cells infected with shTNFAIP1 or shControl lentivirus (lower). c. CCK8 assay was used to determine cell proliferation in MHCC97H cells infected with TNFAIP1 or the control lentivirus (left) (**p<0.01, Student's t-test) and in SMMC7721 cells infected with shTNFAIP1 or shControl lentivirus (right) (**p < 0.01, one-way ANOVA) at 24, 48, 72 and 96 h. d. Representative photographs of the tumors at 6 weeks after injection with MHCC97H-TNFAIP1 or Control stable cells (n = 5/group). e. Tumor weight and tumor volume of nude mice subcutaneous injected with MHCC97H-TNFAIP1 or MHCC97H—Control stable cells were measured (n = 5/group) (**P<0.01, Student's t-test). f. Representative photographs of the tumors at 6 weeks after injection with SMMC7721-shTNFAIP1 or shControl stable cells (n = 5/group). g. Tumor weight and tumor volume of nude mice subcutaneous injected with SMMC7721-shTNFAIP1 or SMMC7721-shControl stable cells were measured (n = 5/group) (*P<0.05, Student's t-test). h. Immunostaining of xenograft tumors from MHCC97H-TNFAIP1 and MHCC97H—Control groups (upper) or from SMMC7721-shTNFAIP1 and SMMC7721-shControl groups (lower) were conducted using a specific anti-Ki67 antibody, Scale bars, 25 μm. i. The Ki67-positive cells were quantitatively analyzed in MHCC97H-TNFAIP1 and MHCC97H—Control groups (left) (***P<0.001, Student's t-test) or in SMMC7721-shTNFAIP1 and SMMC7721-shControl groups (Right), (**P<0.01, Student's t-test) (n = 5). j. TUNEL assay to determine cell apoptosis in MHCC97H cells infected with TNFAIP1 or the control lentivirus (upper) and in SMMC7721 cells infected with shTNFAIP1 or shControl lentivirus (lower). Scale bar, 25 μm. k. Quantitative analysis of TUNEL staining in MHCC97H cells infected with TNFAIP1 or the control lentivirus (**P<0.01, Student's t-test) and in SMMC7721 cells infected with shTNFAIP1 or shControl lentivirus (**P<0.01, Student's t-test). l. RT-qPCR analysis of the mRNA level of TNFAIP1, RhoB, Bcl-XL and Bcl-2 in MHCC97H cells infected with TNFAIP1 or the control lentivirus and in SMMC7721 cells infected with shTNFAIP1 or shControl lentivirus (*P<0.05, **P<0.01 and ***P<0.001, Student's t-test). m. Western blot analysis of the expression of Cleaved-caspase3, Bcl2, Bcl-XL, Bax, RhoB and TNFAIP1 in MHCC97H infected with TNFAIP1 or the control lentivirus and in SMMC7721 infected with shTNFAIP1 or shControl lentivirus. Data are presented as means ± SEM from triplicate independent experiments. P-values were determined by two-tailed Student's t-test or one-way ANOVA (*P < 0.05, **P < 0.01, ***P < 0.001).

RT-qPCR and Western blot assay showed that TNFAIP1 was overexpressed or was knocked down in HUVECs cells by infected with TNFAIP1 lentivirus or shTNFAIP1 lentivirus (Supplementary Figure S2 a-d). We found that TNFAIP1 overexpression inhibited the capillary tube formation, as the number of branch points and the length of tubes were significantly decreased compared with the control group (Fig. 4c). In contrast, shTNFAIP1 lentivirus infected HUVECs cells showed the increased ability of tube formation compared with the control group (Fig. 4d). Subsequently, RT-qPCR and Western blot analysis was used to examine the expression of VEGF, an important

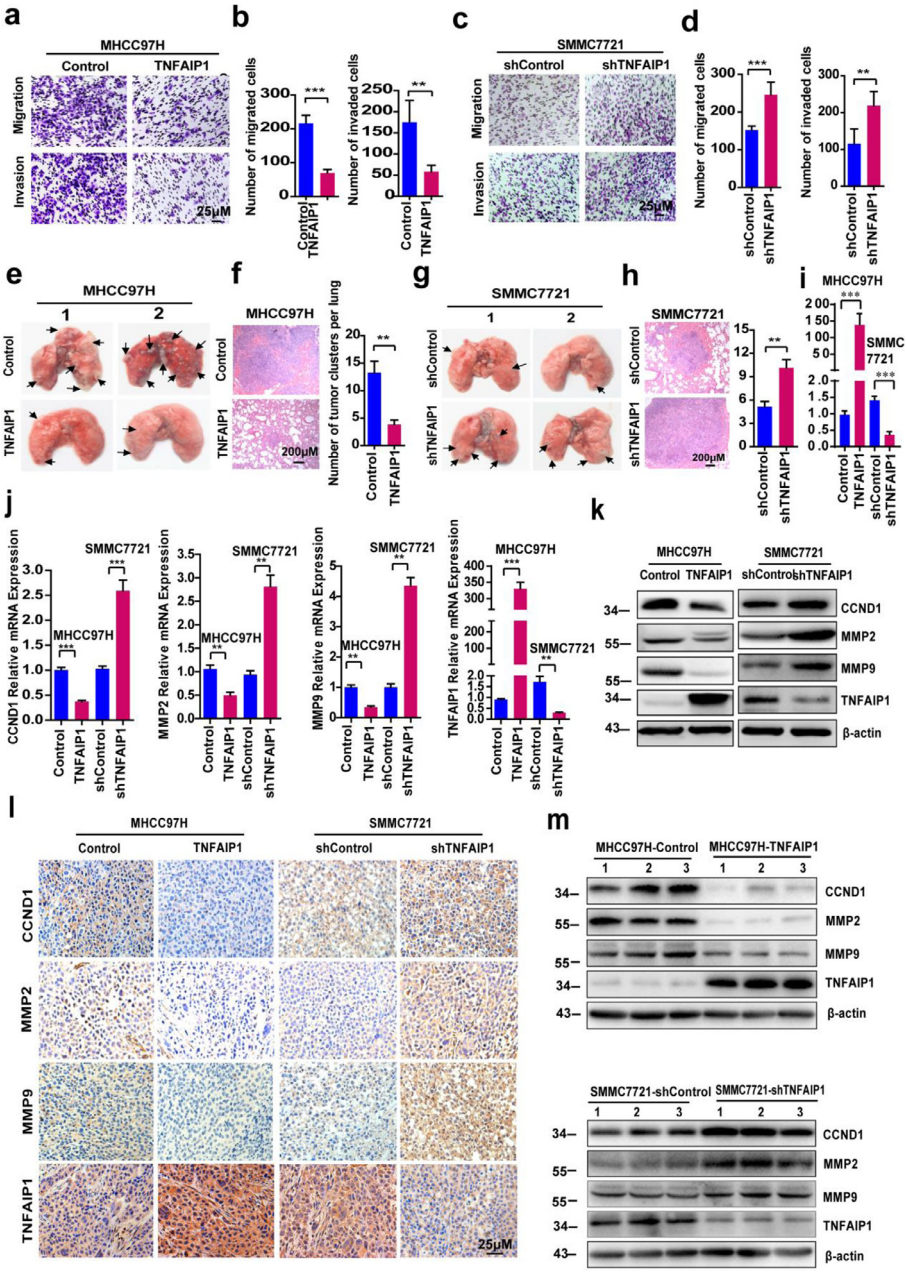

Fig. 3. TNFAIP1 regulates HCC cell migration, invasion and metastasis *in vitro* and *in vivo*. Cell migration and invasion assay for MHCC97H cells infected with TNFAIP1 or the control lentivirus using transwell membranes. a. The migrated and invaded MHCC97H cells were stained with crystal violet. Scale bars, 25 μm. b. The number of migration and invasion of MHCC97H cells was counted and analyzed in five random fields of each filter (**$P < 0.01$, ***$P < 0.001$, Student's *t*-test). Cell migration and invasion assay for SMMC7721 cells infected with shTNFAIP1 or shControl lentivirus using transwell membranes. c. The migrated and invaded SMMC7721 cells were stained with crystal violet. Scale bars, 25 μm. d. The number of migration and invasion of SMMC7721 cells was counted and analyzed in five random fields of each filter (**$P < 0.01$, ***$P < 0.001$, Student's *t*-test). e. Photomicrographs of metastatic lung nodules in nude mice by tail-vein injection of MHCC97H-TNFAIP1 and Control stable cells. The arrows indicate the metastatic nodes on the surface of the lung ($n = 7$/group). f. Lung nodules were stained by hematoxylin and eosin (H&E) staining kit and the number of lung metastatic foci in each group was calculated ($n = 7$) (**P<0.01, Student's *t*-test). Scale bar, 200 μm. g. Photomicrographs of metastatic lung nodules in nude mice by tail-vein injection of SMMC7721-shTNFAIP1 and shControl stable cells. The arrows indicate the metastatic nodes on the surface of the lung ($n = 7$/group). h. Lung nodules were stained by H&E staining kit and the number of lung metastatic foci in each group was calculated ($n = 7$) (**$P < 0.01$, Student's *t*-test). Scale bar, 200 μm. i. RT-qPCR analysis of the mRNA level of TNFAIP1 in lungs of nude mice (***$P < 0.001$, Student's *t*-test). j. RT-qPCR analysis of the mRNA level of CCND1, MMP2, MMP9 and TNFAIP1 in MHCC97H cells infected with TNFAIP1 or the control lentivirus and in SMMC7721 cells infected with shTNFAIP1 or shControl lentivirus (**$P < 0.01$, ***$P < 0.001$, Student's *t*-test). k. Western blot analysis of the protein expression of CCND1, MMP2, MMP9 and TNFAIP1 in MHCC97H infected with TNFAIP1 or the control lentivirus and in SMMC7721 infected with shTNFAIP1 or shControl lentivirus. l. Immunostaining of xenograft tumors from MHCC97H-TNFAIP1, MHCC97H—Control, SMMC7721-shTNFAIP1 and SMMC7721-shControl groups were conducted using a specific anti-CCND1, MMP2, MMP9 or TNFAIP1 antibodies (DAB staining, brown) and counterstained with haematoxylin (blue) ($n = 5$/group). Scale bar, 25 μm. m. Western blot was performed on the same tumor samples for detection of CCND1, MMP2, MMP9 and TNFAIP1. Data are presented as means ± SEM from triplicate independent experiments. P-values were determined by two-tailed Student's *t*-test (**$P < 0.01$, ***$P < 0.001$).

angiogenesis-associated growth factor [31] in MHCC97H-TNFAIP1 and SMMC7721-shTNFAIP1 stable cells. The results showed that the mRNA and protein levels of VEGF were decreased in MHCC97H-TNFAIP1 stable cells compared to the control cells (Fig. 4e and f). However, a higher level of VEGF was detected in SMMC7721-shTNFAIP1 stable cells compared with control cells (Fig. 4e and f). The results were further confirmed by IHC and Western blot analysis in MHCC97H-TNFAIP1 and SMMC7721-shTNFAIP1 stable cell-derived xenograft tumors (Fig. 4g and h). These results indicate that TNFAIP1 inhibits angiogenesis *in vitro* and *in vivo*.

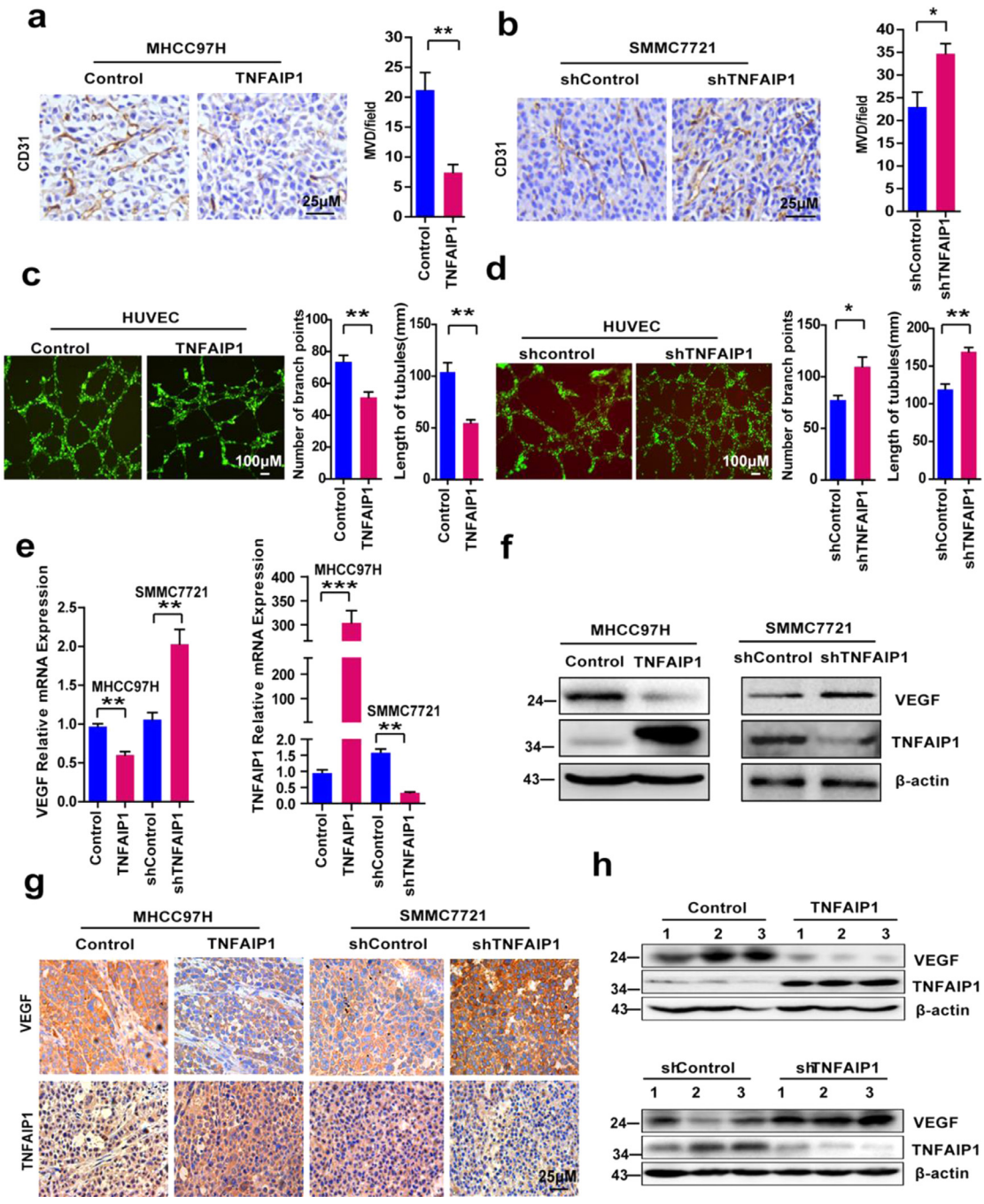

Fig. 4. TNFAIP1 regulates angiogenesis *in vitro* and *in vivo*. a. Tumors from MHCC97H-TNFAIP1 and MHCC97H—Control groups were immunostained with CD31, and the microvessel density (MVD) was calculated in tumors from each group ($n = 5$/group) (**$P < 0.01$, Student's *t*-test). Scale bars, 25 μm. b. Tumors from SMMC7721-shTNFAIP1 and SMMC7721-shControl groups were immunostained with CD31, and the microvessel density (MVD) was calculated in tumors from each group ($n = 5$/group) (*$P < 0.05$, Student's *t*-test). Scale bars, 25 μm. c. HUVEC cells were infected with TNFAIP1 or control lentivirus respectively. The tube formation was observed under a Diaphot Inverted Microscope Camera System (Leica). The number of branch points and the length of tubes were quantified by counting five random fields (**$P<0.01$, Student's *t*-test). Scale bars, 100 μm. d. HUVEC cells were infected with shTNFAIP1 or shControl lentivirus respectively. The tube formation was observed under a Diaphot Inverted Microscope Camera System (Leica). The number of branch points and the length of tubes were quantified by counting five random fields (*$P < 0.05$, **$P<0.01$, Student's *t*-test). Scale bars, 100 μm. e. RT-qPCR analysis of the mRNA levels of VEGF and TNFAIP1 in MHCC97H cells infected with TNFAIP1 or the control lentivirus and in SMMC7721 cells infected with shTNFAIP1 or shControl lentivirus (**$P < 0.01$, ***$P < 0.001$, Student's *t*-test). f. Western blot analysis of the protein expression of VEGF and TNFAIP1 in MHCC97H infected with TNFAIP1 or the control lentivirus and in SMMC7721 infected with shTNFAIP1 or shControl lentivirus. g. Immunostaining of tumors from MHCC97H-TNFAIP1, MHCC97H—Control, SMMC7721-shTNFAIP1 and SMMC7721-shControl groups were conducted using a specific anti-VEGF and TNFAIP1 antibody (DAB staining, brown) and counterstained with haematoxylin (blue) ($n = 5$/group). h. Western blot analysis was performed on the same tumor samples for detection of VEGF and TNFAIP1 expression. Data are presented as means ± SEM from triplicate independent experiments. P-values were determined by two-tailed Student's *t*-test (*$P < 0.05$, **$P < 0.01$, ***$P < 0.001$).

3.5. TNFAIP1 inhibits HCC progression by blocking the trans-activation of NF-κB

CCND1, MMP2, MMP9, and VEGF had been reported to be NF-κB target genes [32–35], and our previous study suggested that TNFAIP1 suppresses the transcriptional activities of NF-κB in HEK293FT [21] and uterine cancer [13] cells, implying that TNFAIP1 may also inhibit the trans-activation of NF-κB in HCC cell. In this study, we found that the NF-κB reporter activities were significantly inhibited in MHCC97H-TNFAIP1 stable cells, but significantly increased in

SMMC7721-shTNFAIP1 stable cells compared with the control cells (Fig. 5a). Moreover, immunofluorescence staining showed that p65 nuclear signals were markedly decreased in MHCC97H-TNFAIP1 stable cells (Fig. 5b), but dramatically increased in SMMC7721-shTNFAIP1 stable cells (Fig. 5c). Subsequently, we sought to determine how TNFAIP1 inhibits the trans-activation of NF-κB in HCC cell. The results showed that MHCC97H-TNFAIP1 stable cells displayed the decreased expression of p-p65, p-IκBα, and p-IKKα/β, but increased expression of IκBα, in comparison to the control cells. In contrast, the knockdown of TNFAIP1 resulted in the increased levels of p-p65, p-IκBα and p-IKKα/β, but a reduction of IκBα in SMMC7721-shTNFAIP1 stable cells, compared with the control cells (Fig. 5d). Similar results were found in the xenograft tumors induced by MHCC97H-TNFAIP1 stable cells and SMMC7721-shTNFAIP1 stable cells (Fig. 5e). These data indicate that TNFAIP1 decreases the phosphorylation of IKKα/β and IκBα, prevents the degradation of IκBα and the phosphorylation of p65, and eventually leads to the inhibition of the trans-activation of NF-κB.

Various lines of evidence suggest that NF-κB promotes HCC cell proliferation, migration, invasion, and angiogenesis through upregulation of CCND1, MMP2, and VEGF expression by binding to their promoter regions [32–35]. Based on our observation that TNFAIP1 suppresses the trans-activation of NF-κB, we reasoned that TNFAIP1 might inhibit HCC cell proliferation, migration, invasion, and angiogenesis by blocking the trans-activation of NF-κB. To prove our hypothesis, MHCC97H and SMMC7721 cell were infected with shTNFAIP1 and shControl lentiviral particles to generate MHCC97H-shTNFAIP1 and SMMC7721-shTNFAIP1 stable cells, and treated with pyrrolidine dithiocarbamic acid (PDTC, a NF-κB inhibitor) for 48 h. After 48 h, the mRNA levels of CCND1, MMP2, and VEGF were determined. The results showed that the knockdown of TNFAIP1 upregulated the mRNA levels of CCND1, MMP2, and VEGF, but the effect was largely abolished after treatment with PDTC (Fig. 5f and g). Taken together, these findings indicate that TNFAIP1 inhibits HCC progression by blocking the trans-activation of NF-κB.

3.6. TNFAIP1 interacts with CSNK2B and promotes its ubiquitin-mediated degradation and suppresses CSNK2B-dependent NF-κB trans-activation

To further elucidate the molecular mechanism underlying the inhibitory effect of TNFAIP1 on the trans-activation of NF-κB, Co-IP assay coupled with LC-MS/MS assay was used to identify TNFAIP1-interaction proteins in HCC cells. CSNK2B, a regulatory subunit of CK2 was identified (Fig. 6a). Interestingly, our previous study had reported that CSNK2B was implicated in binding and phosphorylation of TNFAIP1 [20], indicating that CSNK2B is an important TNFAIP1-associated protein. The interaction between endogenous TNFAIP1 and CSNK2B in MHCC97H cells (Fig. 6b) or tagged TNFAIP1 and CSNK2B in HEK293FT cells (Fig. 6c) was verified by Co-IP. Furthermore, the glutathione S-transferase (GST) pull-down assay showed that the region spanning residues 97–316 of TNFAIP1 was required for the direct interaction with CSNK2B (Fig. 6d). Taken together, these results indicate that TNFAIP1 directly interacts with CSNK2B.

To investigate whether TNFAIP1 regulates CSNK2B protein levels, TNFAIP1 plasmid was transfected into MHCC97H cells in a dose-dependent manner. Western blot analysis indicated that TNFAIP1 dose-dependently decreased CSNK2B protein expression in MHCC97H cells (Fig. 6e). To investigate whether TNFAIP1 induces CSNK2B degradation by affecting its protein stability, the protein half-life of CSNK2B in MHCC97H-TNFAIP1 stable cells and control cells were analyzed. The results revealed that the degradation rate of CSNK2B was much more rapid in MHCC97H-TNFAIP1 stable cells than that in the control cells (Fig. 6f). TNFAIP1 is a BTB domain-containing protein, which serves as a substrate adaptor for cullin3 (Cul3)-based ubiquitin ligases and mediates ubiquitination degradation of some proteins via a Cul3/TNFAIP1 ubiquitin ligase complex [8,36]. To investigate whether CSNK2B is a substrate of the Cul3/TNFAIP1 ubiquitin ligase complex, the MHCC97H-TNFAIP1 stable cells and control cells were treated with a proteasome inhibitor, MG132. The results showed that TNFAIP1-induced CSNK2B down-regulation was rescued by treatment with MG132 (Fig. 6g). Subsequently, the effect of knockdown of TNFAIP1 on the endogenous interaction between CSNK2B and Cul3 was investigated. The results showed that the interaction between CSNK2B and Cul3 was significantly attenuated in MHCC97H by infecting with shTNFAIP1 lentiviral particles (Fig. 6h), indicating that TNFAIP1 may induce CSNK2B degradation via the Cul3/TNFAIP1 ubiquitin ligase complex. To further confirm the results, we examined the effect of knockdown of Cul3 or TNFAIP1 on CSNK2B stability in MHCC97H cells by infecting with shCul3 or shTNFAIP1 lentiviral particles. As expected, the knockdown of Cul3 or TNFAIP1 caused significantly increased expression of CSNK2B (Fig. 6i and j). We further examined the level of CSNK2B ubiquitination, and found that the knockdown of TNFAIP1 significantly decreased CSNK2B ubiquitination in MHCC97H by infecting with TNFAIP1-shTNFAIP1 lentiviral particles (Fig. 6k). Furthermore, we also observed that co-expression of Cul3 and TNFAIP1 potentiated CSNK2B ubiquitination in combination with Rbx1 (the catalytic subunit of Cul3 family ligases) and ubiquitin plasmids in HEK293FT cells (Fig. 6l). Taken together, these data indicate that TNFAIP1 induced degradation of CSNK2B via the Cul3/TNFAIP1 ubiquitin ligase complex.

Previous studies have indicated that CK2 promotes aberrant activation of NF-κB in many cancers by directly phosphorylating IKK, IκBα, and p65 [37–39]. According to our previous conclusions, we supposed that TNFAIP1 inhibited the trans-activation of NF-κB by down-regulating CSNK2B. Firstly, we found that CSNK2B dose-dependently enhanced NF-κB reporter activities in MHCC97H cells (Fig. 6m). Moreover, we observed that CSNK2B overexpression led to an increase in the expression of CCND1, MMP2, and VEGF, and also the phosphorylation of IκBα (Ser 32), IKKα/β (Ser 176/180), p65 (Ser536), and p65 (Ser529) in both MHCC97H and SMMC7721 cells (Fig. 6o). These data suggested that CSNK2B plays an important role in the activation of NF-κB pathway. To further confirm our hypothesis, MHCC97H cells were infected with shTNFAIP1 or shCSNK2B or shControl and co-transfected with NF-κB luciferase reporter plasmid. Luciferase reporter assay showed that knockdown of TNFAIP1 significantly activated NF-κB reporter activity, whereas, the effect was abolished by silencing CSNK2B (Fig. 6n). Moreover, Western blot analysis showed that knockdown of CSNK2B markedly attenuated the phosphorylation levels of p65 (Ser536) and p65 (Ser529), as well as the expression of the NF-κB target proteins, including CCND1, MMP2, and VEGF, induced by knockdown of TNFAIP1 in both MHCC97H and SMMC7721 cells (Fig. 6p). In conclusion, these data indicate that TNFAIP1 inhibits trans-activation of NF-κB through selective downregulation of CSNK2B.

3.7. CSNK2B reverses the anti-carcinogenic effect of TNFAIP1

CSNK2B has been found to regulate cell proliferation, migration, invasion, and angiogenesis by activating the trans-activation of NF-κB in Head and Neck Cancer [19]. To investigate whether the anti-carcinogenic effect of TNFAIP1 is mediated by down-regulation of CSNK2B, MHCC97H and SMMC7721 cells were infected with TNFAIP1 or TNFAIP1/CSNK2B lentiviral particles. Western blot assay showed that TNFAIP1 and CSNK2B were overexpressed in MHCC97H and SMMC7721 cells (Supplementary Figure S3 a and b). CCK8 assay showed that co-expression of CSNK2B and TNFAIP1 significantly attenuated the inhibitory effect of TNFAIP1 on MHCC97H and SMMC7721 cells proliferation (Fig. 7a). Similarly, transwell assay showed that co-expression of CSNK2B and TNFAIP1 in MHCC97H and

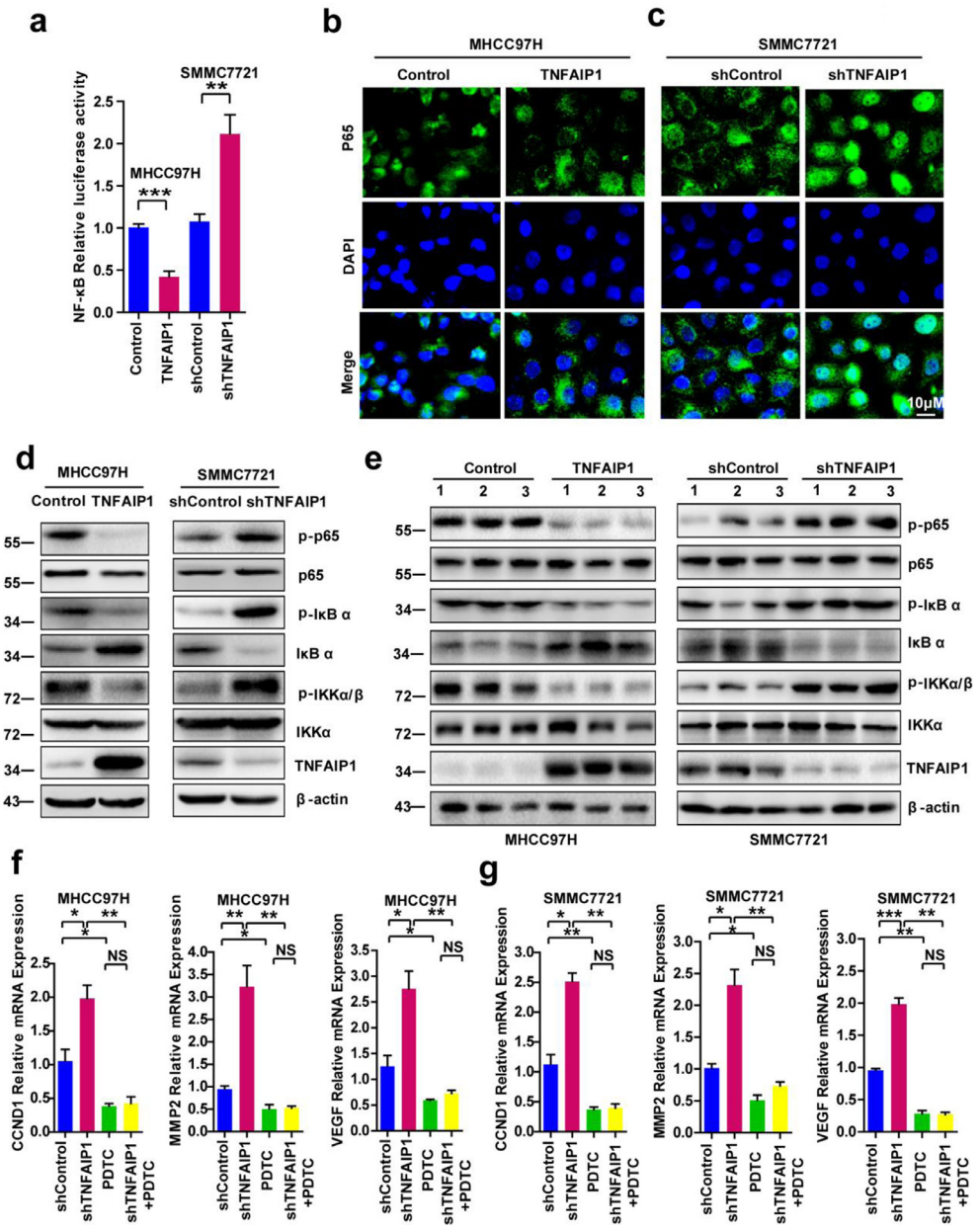

Fig. 5. TNFAIP1 inhibits the trans-activation of NF-κB. a. The luciferase activity was detected in MHCC97H cells infected with TNFAIP1 or the control lentivirus and in SMMC7721 cells infected with shTNFAIP1 or shControl lentivirus by co-transfected with NF-κB luciferase reporter plasmid. Relative luciferase activities represent mean ± SEM from triplicate independent experiments (**$P < 0.01$, ***$P < 0.001$, Student's *t*-test). b. Immuofluorescence microscopy staining p65 antibody in MHCC97H cells infected with TNFAIP1 or the control lentivirus, the green signal represents p65 staining and blue signal represents nuclear DNA staining by DAPI. Scale bar, 10 μm. c. Immunofluorescence microscopy staining p65 antibody in SMMC7721 cells infected with shTNFAIP1 or shControl lentivirus, the green signal represents p65 staining and blue signal represents nuclear DNA staining by DAPI. Scale bar, 10 μm. d. Western blot analysis of p65, p-p65, IκBα, p-IκBα, IKKα/β and p-IKKα/β in MHCC97H cells infected with TNFAIP1 or the control lentivirus and in SMMC7721 cells infected with shTNFAIP1 or shControl lentivirus. e. Tumors from MHCC97H-TNFAIP1, MHCC97H—Control, SMMC7721-shTNFAIP1 and SMMC7721-shControl groups were used to detect the expression of p65, p-p65, IκBα, p-IκBα, IKKα/β and p-IKKα/β. f. RT-qPCR analysis of the mRNA levels of CCND1, MMP2 and VEGF in MHCC97H cells infected with shControl or shTNFAIP1 lentivirus and treated with PDTC (20 μM) (*$P < 0.05$, **P<0.01, Student's *t*-test). g. RT-qPCR analysis of the mRNA levels of CCND1, MMP2 and VEGF in SMMC7721 cells infected with shControl or shTNFAIP1 lentivirus and treated with PDTC (*P<0.05, **$P < 0.01$, ***P<0.001, Student's *t*-test). Data are presented as means ± SEM from triplicate independent experiments. P-values were determined by two-tailed Student's *t*-test (*$P < 0.05$, **$P < 0.01$, ***$P < 0.001$).

SMMC7721 cells counteracted TNFAIP1-inhibited migration *in vitro* (Fig. 7b and c). To further confirm this conclusion, MHCC97H-TNFAIP1, MHCC97H-TNFAIP1-CSNK2B, SMMC7721-TNFAIP1, SMMC7721-TNFAIP1-CSNK2B and Control stable cells were constructed by infecting with TNFAIP1 or TNFAIP1/CSNK2B lentiviral particles, and were intravenously injected into 4-week-old female nude mice through the tail vein. The result showed that co-expression of CSNK2B and TNFAIP1 in MHCC97H and SMMC7721 cells counteracted TNFAIP1-inhibited lung metastasis *in vivo* (Fig. 7d-f). Western blot assay showed that TNFAIP1 or CSNK2B was overexpressed in lungs of nude mice by infected with TNFAIP1 or CSNK2B stable cells (Supplementary Figure S3 c and d). Moreover, we also observed that co-expression of CSNK2B and TNFAIP1 abrogated the inhibitory effect of TNFAIP1 on tube formation in HUVECs cells by infecting with TNFAIP1 or TNFAIP1/CSNK2B lentiviral particles *in vitro* (Fig. 7g and h). Furthermore, we further analyzed the reciprocal relationship between TNFAIP1 and CSNK2B in clinical HCC samples. IHC analysis shows that TNFAIP1 was negatively correlated with CSNK2B expression (Supplementary Figure S4). Altogether, these data suggest that TNFAIP1 suppresses the trans-activation of NF-κB

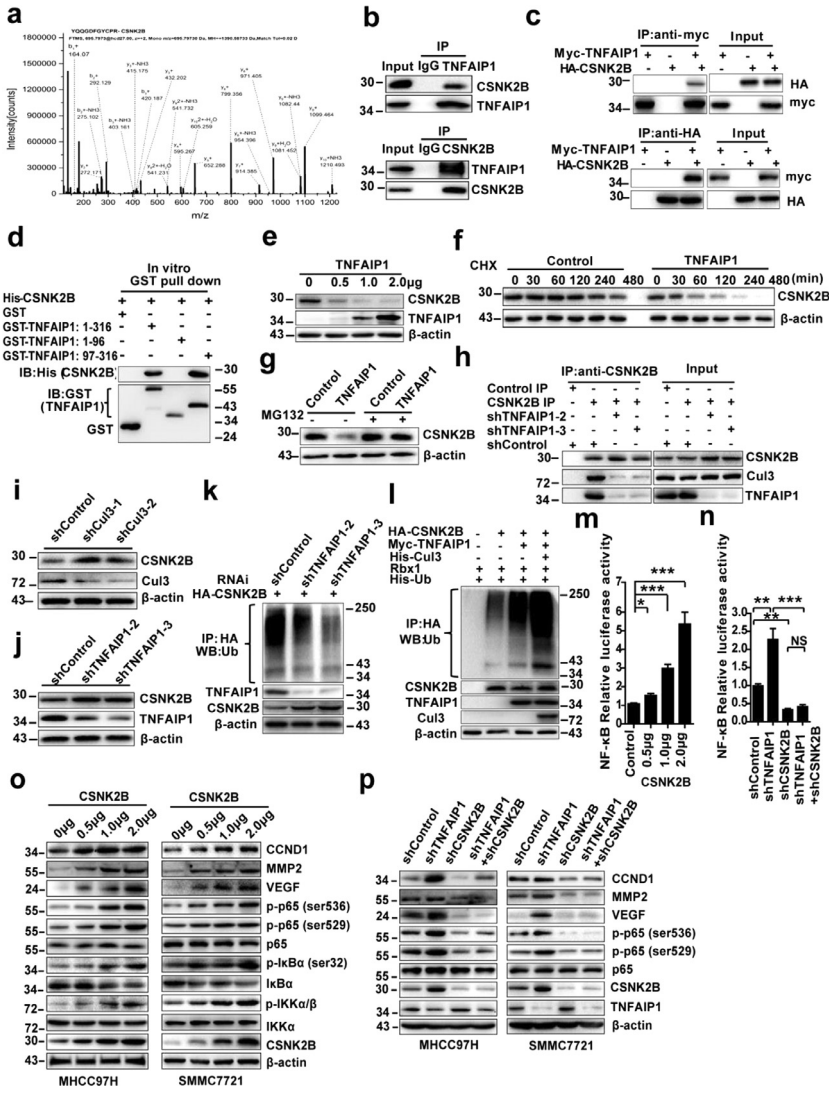

Fig. 6. TNFAIP1 accelerated CSNK2B's ubiquitin-mediated degradation and inhibited CSNK2B-dependent NF-κB trans-activation. a. Whole-cell extracts from MHCC97H cells transfected with Myc-tagged TNFAIP1 plasmid and subjected to incubate with anti-Myc antibody. The purified protein was analyzed by LC-MS/MS analysis. b. Western blot analysis of the whole-cell lysates (input) and Co-IP complex captured with anti-TNFAIP1 antibody (Upper panel) and anti-CSNK2B (lower panel) in MHCC97H cells. c. Western blot analysis of the indicated proteins in the input and Co-IP complex captured with anti-Myc (Upper panel) and anti-HA antibodies (lower panel) in HEK293FT cells transfected with Myc-tagged TNFAIP1 and HA-tagged CSNK2B. d. Western blot analysis of CSNK2B in GST pull-down complex by recombinant GST alone or GST-tagged TNFAIP1 (1−316), GST-tagged TNFAIP1 (1−96), GST-tagged TNFAIP1 (97−316) and His-CSNK2B proteins. e. Western blot analysis of CSNK2B level in MHCC97H cells transfected with TNFAIP1 plasmid (0 μg, 0.5 μg, 1.0 μg and 2.0 μg). f. Western blot analysis of CSNK2B level in MHCC97H-TNFAIP1 stable cells and control cells after treatment with cycloheximide. g. Western blot analysis of CSNK2B level in MHCC97H-TNFAIP1 stable cells and control cells after treatment with MG132. h. Immunoprecipitation analysis of the interaction between TNFAIP1, CSNK2B and Cul3 in MHCC97H cells infected with shTNFAIP1 or shControl lentivirus. i. Western blot analysis of CSNK2B level in MHCC97H cells infected with shCul3 or shControl lentivirus. j. Western blot analysis of CSNK2B levels in MHCC97H cells infected with shTNFAIP1 or shControl lentivirus. k. Immunoprecipitation analysis for CSNK2B ubiquitination in MHCC97H cells infected with shControl or shTNFAIP1 lentivirus. l. Immunoprecipitation analysis for CSNK2B ubiquitination in HEK293FT cells transfected with indicated constructs. m. CSNK2B mediates the activation of NF-κB. The luciferase activity was detected in MHCC97H cells by co-transfected with CSNK2B plasmid (0 μg, 0.5 μg, 1.0 μg and 2.0 μg) and NF-κB luciferase reporter plasmid (2.0 μg), relative luciferase activities represent mean ± SEM from triplicate independent experiments ($^{*}P < 0.05$, $^{***}P < 0.001$, Student's t-test). n. The luciferase activity was detected in MHCC97H cells infected with shTNFAIP1 or shCSNK2B or shControl, relative luciferase activities represent mean ± SEM from triplicate independent experiments ($^{**}P < 0.01$, $^{***}P < 0.001$, Student's t-test). o. Western blot analysis of CCND1, MMP2, VEGF, p65, p-p65 (ser536), p-p65 (ser529), p-IκBα (ser32), IκBα, p-IKKα/β (ser176/180), IKKα, CSNK2B and β-actin in MHCC97H cells and in SMMC7721 cells transfected with CSNK2B plasmid (0 μg, 0.5 μg, 1.0 μg and 2.0 μg). p. Western blot analysis of CCND1, MMP2, VEGF, p65, p-p65 (ser536), p-p65 (ser529), CSNK2B, TNFAIP1 and β-actin in MHCC97H cells and in SMMC7721 cells infected with shTNFAIP1 or shCSNK2B or shControl lentivirus. Data are presented as means ± SEM from triplicate independent experiments. P-values were determined by two-tailed Student's t-test ($^{*}P < 0.05$, $^{**}P < 0.01$, $^{***}P < 0.001$).

by down-regulation of CSNK2B, whereas CSNK2B overexpression reverses the anti-carcinogenic effect of TNFAIP1 in HCC (Fig. 7i).

4. Discussion

Although TNFAIP1 has been reported to be involved in the progression of many cancers [9,14,30,40], the regulatory roles of TNFAIP1 in HCC and the molecular mechanism remains largely unknown. In this study, our results showed that TNFAIP1 is specifically downregulated in HCC clinical samples and cells; and that overexpression of TNFAIP1 inhibits HCC cell proliferation, migration, invasion, metastasis, and angiogenesis through selectively downregulating CSNK2B via the ubiquitin-mediated degradation pathway, which then blocks NF-κB trans-activation (Fig. 7i). Therefore, we have identified TNFAIP1 as a potential therapeutic target of HCC, and our study provides insight into the role of TNFAIP1 in HCC pathogenesis and suggests that the TNFAIP1/CSNK2B/NF-κB pathway could be a putative therapeutic target in HCC.

Along with other studies, our findings suggest that TNFAIP1 is a multi-faceted tumor suppressor in many cancers. In this study, we

elucidated the significant impact of TNFAIP1 on the inhibition of HCC cell proliferation, migration, invasion, angiogenesis, and induction of apoptosis. Consistently, we had previously reported that TNFAIP1 inhibits growth and invasion, induces apoptosis in uterine cancer [13], and attenuates proliferation of gastric carcinoma [14]. Moreover, TNFAIP1 has been shown to promote apoptosis of HeLa cells [9]. Recently, emerging evidence has identified TNFAIP1 as a critical target for the inhibition of cell proliferation, migration, and invasion of NSCLC [6,7,40] and pancreatic cancer [41]. Therefore, these findings regarding the multi-faceted inhibitory role of TNFAIP1 in HCC, NSCLC, gastric carcinoma, cervical carcinoma, and pancreatic cancer suggest that TNFAIP1 is potentially important for the development of therapeutics for these cancers. However, it is worth noting that TNFAIP1 has also been reported to induce cell growth and inhibit apoptosis in osteosarcoma cells [30], as well as mediate cell migration in MDA-MB231 human mammary carcinoma cells [5]. The exact molecular mechanisms underlying the different roles of TNFAIP1 in various cancers still remain to be elucidated. It is possible that TNFAIP1 may dynamically regulate different cancers, or be determined by different interactors under distinct cellular contexts in different cancers to finally contribute to various intracellular events.

Our previous study reported that TNFAIP1 induces apoptosis and exerts an inhibitory effect on cell proliferation and invasion in uterine cancer cells through downregulating the NF-κB pathway [13]. In the present study, we demonstrated that in HCC, TNFAIP1 is also a potent inhibitor of NF-κB, an important transcription factor that has been reported to be involved in driving angiogenesis and metastasis of HCC [35]. The molecular mechanisms regarding the role of NF-κB in regulating angiogenesis and metastasis have been well studied. It is well known that NF-κB can upregulate MMP2 and MMP9 expression via directly binding to their promoter regions, which belongs to the family of zinc-dependent endopeptidases that degrade almost all extracellular matrix components and plays vital roles in promoting cancer invasion and metastasis [33,34]. Moreover, NF-κB can promote angiogenesis by binding to the VEGF promoter and triggering its transcription [42]. NF-κB has also been reported to control cell growth and differentiation through transcriptional regulation of CCND1 [32]. In the present study, we found that TNFAIP1 dramatically downregulates NF-κB target genes, including CCND1, MMP2, MMP9, and VEGF, strongly suggesting that TNFAIP1 inhibits cell proliferation, angiogenesis, and metastasis via suppressing trans-activation of NF-κB.

Although we previously reported that TNFAIP1 inhibits the transcriptional activities of NF-κB via binding and promoting the degradation of KCTD10 [21], the exact molecular mechanisms underlying the role of TNFAIP1 in inhibiting NF-κB remains poorly understood, which led us to identify NF-κB-associated proteins that were bound and regulated by TNFAIP1. Our previous studies revealed the interaction of TNFAIP1 with CSNK2B [20]. In this study, we further identified CSNK2B as a binding protein using Co-IP coupled with LC-MS/MS analysis. Previous studies have shown that CK2 can mediate the activation of NF-κB induced by serum factors via phosphorylating the IKK complex and promoting IκBα (a NF-κB endogenous inhibitor) degradation and releasing p65 Ser536/p50 [17]. Moreover, CK2 induced phosphorylation of IκBα at Ser-283, Ser-289, Ser-293, and Thr-291, as well as phosphorylation of p65 at Ser529 to activate NF-κB directly [38,43]. Therefore, CK2 subunits are critical to controlling trans-activation of NF-κB. Considering significant overexpression of CK2α and CK2β has been found in HCC [44], and CK2 has been reported to be closely associated with HCC cell apoptosis, proliferation, migration and invasion [45–47], it is reasonable to question whether CSNK2B is implicated in the TNFAIP1-mediated inhibitory effect on NF-κB trans-activation and HCC cell proliferation, migration, invasion, and angiogenesis. In the present study, we found that: (1) Over-expression of CSNK2B significantly enhanced trans-activation of NF-κB in a dose-dependent manner in HCC cell; (2) CSNK2B silencing attenuated TNFAIP1 knockdown-induced trans-activation of NF-κB in HCC cell; and (3) CSNK2B over-expression reversed the anti-carcinogenic effect of TNFAIP1 in the progression of HCC cell proliferation, migration, and angiogenesis. These results strongly suggest that TNFAIP1 is a primary negative regulator of CSNK2B, and thereby inhibits trans-activation of NF-κB and subsequently restricts HCC cell proliferation, metastasis, and angiogenesis (Fig. 7i).

Another important finding is that CSNK2B was identified as a novel substrate of TNFAIP1/Cul3 ubiquitination protein complexes. It has been well documented that TNFAIP1 is an evolutionarily conserved BTB adapter for Cul3-mediated ubiquitination-dependent protein degradation. For example, TNFAIP1 can be recruited to Cul3-based ubiquitin ligase complexes, specifically promoting the ubiquitination and degradation of RhoA, thereby affecting actin cytoskeleton structure and cell movement [8]. In addition, TNFAIP1/Cul3 ubiquitination protein complexes have been implicated in estrogen-related receptor α (ERRα)-triggered RhoA instability and impaired cell migration [5]. Therefore, it would be interesting to investigate whether CSNK2B is a novel substrate that would be ubiquitinated and degraded by TNFAIP1/Cul3 ubiquitination protein complexes. In this study, we found that silencing of endogenous TNFAIP1 or Cul3 markedly increased CSNK2B protein expression, and knockdown of TNFAIP1 attenuated the binding of CSNK2B to Cul3, as well as ubiquitination of CSNK2B. Moreover, co-expression of Cul3, TNFAIP1, and ubiquitin in HEK293FT cells significantly potentiated polyubiquitination of CSNK2B. In addition, it is worth noting that we also identified Isoform 2 of Cul3 and ubiquitin-conjugating enzyme E2 as CSNK2B-interacting proteins using Co-IP combined with LC-MS/MS analysis (Supplementary Table S3). These studies suggest that TNFAIP1 is a vital adaptor protein for mediating the assembly of substrate protein, CSNK2B, into Cul3 ubiquitination protein complexes for ubiquitination. However, whether TNFAIP1/Cul3 ubiquitination protein complexes mediate K48-linked ubiquitination of CSNK2B still remains to be determined.

Regarding KCTD10, a member of the TNFAIP1 family, KCTD10 also contains a highly conserved BTB domain, which is generally thought to mediate homo- or heterotypic interactions [48]. Our previous study reported that KCTD10 is involved in regulating the inhibitory effect of TNFAIP1 on transcriptional activities of NF-κB [21]; thus, it is possible that KCTD10 may also be implicated in regulating CSNK2B stability through binding to TNFAIP1/Cul3 ubiquitination protein complexes. Although the role of KCTD10 has not been investigated in the present study, KCTD10 has been reported to be an adaptor of the Cul3/KCTD10 E3 complex and was essential for RhoB degradation in human epidermal growth factor receptor 2 (EGF2)-positive breast cancer cells [49]. Therefore, KCTD10 binds to TNFAIP1, perhaps to afford multiple substrate orientations within the same Cul3 ubiquitination protein complex in order to regulate the substrate dynamically. This issue will be further investigated in the future.

In summary, we have identified TNFAIP1 as a critical negative regulator that controls multiple facets essential for HCC proliferation, metastasis, and angiogenesis. In particular, we showed that the anti-carcinogenic effect of TNFAIP1 involves the induction of CSNK2B ubiquitination and degradation via formation of TNFAIP1/Cul3 ubiquitination protein complexes, subsequently leading to the inhibition of NF-κB and its downstream target genes, including MMP2/MMP9, VEGF, and CCND1. This study also demonstrated that TNFAIP1 might be a novel marker for the prognosis of HCC and a potential therapeutic target. Elevation of the expression of TNFAIP1 might be beneficial for HCC treatment in the clinic.

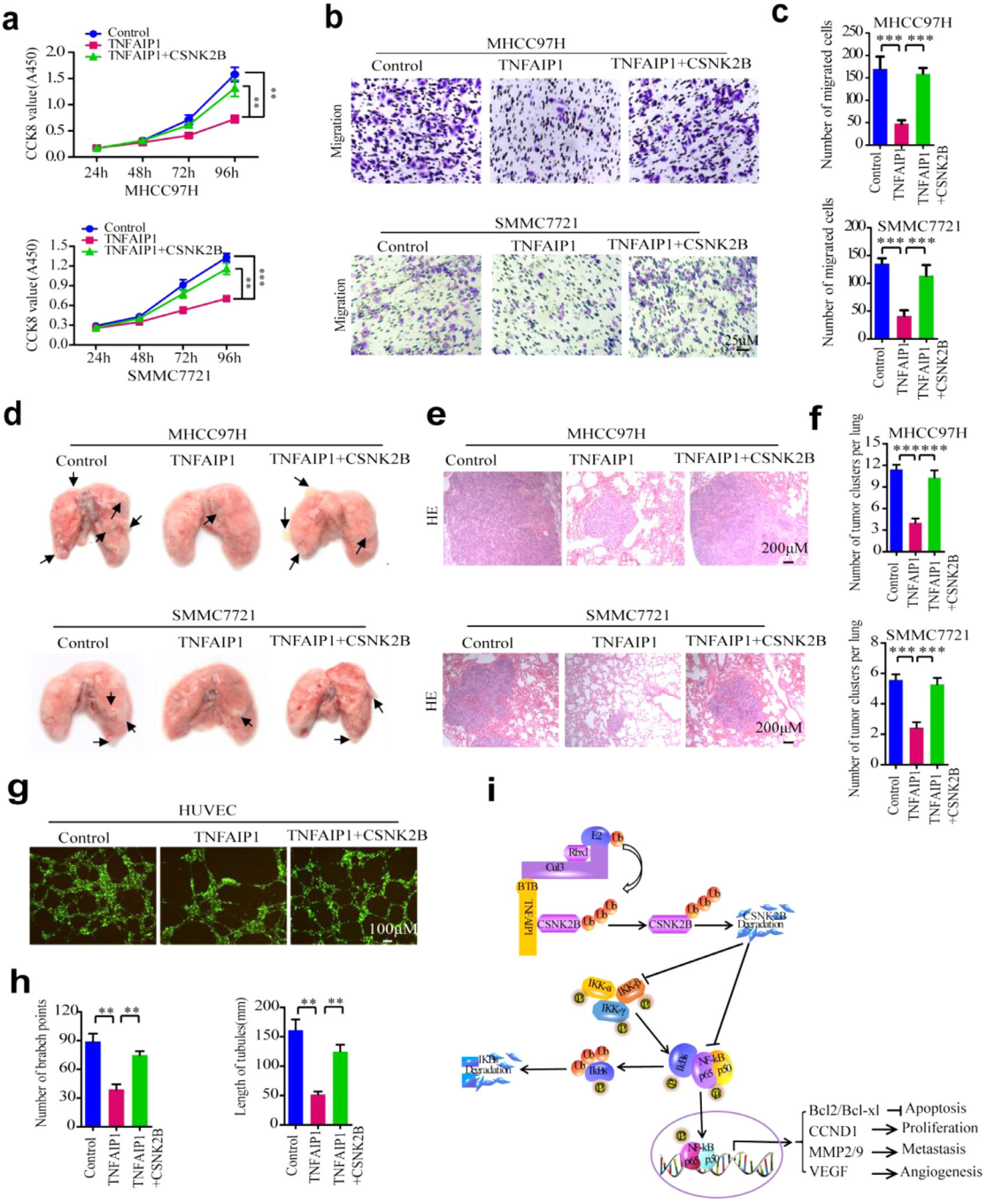

Fig. 7. CSNK2B reverses the anti-carcinogenic effect of TNFAIP1. a. CCK8 assay to determine cell proliferation in MHCC97H cells (upper) or in SMMC7721 cells (lower) were infected with TNFAIP1 or TNFAIP1/CSNK2B and Control lentiviral particles at 24, 48, 72 and 96 h (**$P < 0.01$, ***$P < 0.001$, Student's *t*-test). b. Cell migration assay for MHCC97H cells (upper) and SMMC7721 cells (lower) were infected with TNFAIP1 or TNFAIP1/CSNK2B and Control lentiviral particles using transwell membranes. Scale bars, 25 μm. c. The migrated cells were stained with crystal violet and the number of cell migration was counted in five random fields of each filter (***$P < 0.001$, Student's *t*-test). d. Photomicrographs of metastatic lung nodules in nude mice by tail-vein injection of MHCC97H-TNFAIP1, MHCC97H-TNFAIP1-CSNK2B and Control stable cells (upper), and SMMC7721-TNFAIP1, SMMC7721-TNFAIP1-CSNK2B and Control stable cells (lower). The arrows indicate the metastatic nodes on the surface of the lung ($n = 7$/group). e. Lung nodules were stained by hematoxylin and eosin (H&E) staining kit and the number of lung metastatic foci in each group was calculated (f) ($n = 7$/group) (***$P < 0.001$, Student's *t*-test). Scale bar, 200 μm. g. HUVEC cells were infected with TNFAIP1 or TNFAIP1/CSNK2B lentiviral particles. The tube formation was observed under a Diaphot Inverted Microscope Camera System (Leica). Scale bar, 100 μm. h. The number of branch points and the length of the tube were quantified by counting five random fields (**$P < 0.01$, Student's *t*-test). i. The schematic diagram shows the effect of TNFAIP1 on HCC cell proliferation, apoptosis, metastasis and angiogenesis through suppression of the CSNK2B/NF-κB signaling. Data are presented as means ± SEM from triplicate independent experiments. P-values were determined by two-tailed Student's *t*-test (**$P < 0.01$, ***$P < 0.001$).

Funding sources

This work was supported in part by the financial support from the China Natural Science Foundation (No. 81972642, No. 81601122 and No. 81770389), Hunan Natural Science Foundation (No. 2017JJ3205), Cooperative Innovation Center of Engineering and New Products for Developmental Biology of Hunan Province (No. 20134486), and the Scientific Research Fund of Hunan Provincial Education Department (17B162).

Author contributions statement

YX, NL, and S-LX designed the experiments. YX performed the most experiments and wrote the manuscript. NL, S-LX, X-FD, C-XW, and XH revised the manuscript. S-LH and FQ performed the tumor formation assay and some cell and molecular experiments. YS and Z-JZ collected hepatocellular carcinoma tumor tissues and corresponding peritumor tissues and performed immunohistochemical study. C-XW, XH, WC and KW analyzed and interpreted the data. S-WL, L-NX, and YX helped with some cell and molecular experiments.

Declaration of competing interest

There is no conflict of interest for all authors.

Acknowledgments

The authors gratefully thank the Orthopedic Surgery Department at the Second Xiangya Hospital of Central South University for Hepatocellular Carcinoma tumor tissue and corresponding peritumor tissue collection.

Supplementary materials

Supplementary material associated with this article can be found in the online version at doi:10.1016/j.ebiom.2019.102603.

References

[1] Llovet JM, Montal R, Sia D, Finn RS. Molecular therapies and precision medicine for hepatocellular carcinoma. Nat Rev Clin Oncol 2018;15(10):599–616.
[2] Wang R, Zhao N, Li S, Fang JH, Chen MX, Yang J, et al. MicroRNA-195 suppresses angiogenesis and metastasis of hepatocellular carcinoma by inhibiting the expression of VEGF, VAV2, and CDC42. Hepatology 2013;58(2):642–53.
[3] Wolf FW, Marks RM, Sarma V, Byers MG, Katz RW, Shows TB, et al. Characterization of a novel tumor necrosis factor-alpha-induced endothelial primary response gene. J Biol Chem 1992;267(2):1317–26.
[4] Zhou J, Hu X, Xiong X, Liu X, Liu Y, Ren K, et al. Cloning of two rat PDIP1 related genes and their interactions with proliferating cell nuclear antigen. J Exp Zool A Comp Exp Biol 2005;303(3):227–40.
[5] Sailland J, Tribollet V, Forcet C, Billon C, Barenton B, Carnesecchi J, et al. Estrogen-related receptor alpha decreases rhoa stability to induce orientated cell migration. Proc Natl Acad Sci U S A 2014;111(42):15108–13.
[6] Cui R, Kim T, Fassan M, Meng W, Sun HL, Jeon YJ, et al. MicroRNA-224 is implicated in lung cancer pathogenesis through targeting caspase-3 and caspase-7. Oncotarget 2015;6(26):21802–15.
[7] Cui R, Meng W, Sun HL, Kim T, Ye Z, Fassan M, et al. MicroRNA-224 promotes tumor progression in nonsmall cell lung cancer. Proc Natl Acad Sci U S A 2015;112(31):E4288–97.
[8] Chen Y, Yang Z, Meng M, Zhao Y, Dong N, Yan H, et al. Cullin mediates degradation of rhoa through evolutionarily conserved btb adaptors to control actin cytoskeleton structure and cell movement. Mol Cell 2009;35(6):841–55.
[9] Kim DM, Chung KS, Choi SJ, Jung YJ, Park SK, Han GH, et al. RhoB induces apoptosis via direct interaction with TNFAIP1 in hela cells. Int J Cancer 2009;125(11):2520–7.
[10] Lin MC, Lee NP, Zheng N, Yang PH, Wong OG, Kung HF, et al. Tumor necrosis factor-alpha-induced protein 1 and immunity to hepatitis B virus. World J Gastroenterol 2005;11(48):7564–8.
[11] Gladwyn-Ng I, Huang L, Ngo L, Li SS, Qu Z, Vanyai HK, et al. Bacurd1/Kctd13 and bacurd2/tnfaip1 are interacting partners to Rnd proteins which influence the long-term positioning and dendritic maturation of cerebral cortical neurons. Neural Dev 2016;11:7.
[12] Liu N, Yu Z, Xun Y, Li M, Peng X, Xiao Y, et al. TNFAIP1 contributes to the neurotoxicity induced by abeta25-35 in neuro2a cells. BMC Neurosci 2016;17(1):51.
[13] Tan ZW, Xie S, Hu SY, Liao T, Liu P, Peng KH, et al. Caudatin targets tnfaip1/nf-kappab and cytochrome c/caspase signaling to suppress tumor progression in human uterine cancer. Int J Oncol 2016;49(4):1638–50.
[14] Zhou C, Li X, Zhang X, Liu X, Tan Z, Yang C, et al. microRNA-372 maintains oncogene characteristics by targeting TNFAIP1 and affects nfkappab signaling in human gastric carcinoma cells. Int J Oncol 2013;42(2):635–42.
[15] Li F, Zhang J, Arfuso F, Chinnathambi A, Zayed ME, Alharbi SA, et al. NF-kappaB in cancer therapy. Arch Toxicol 2015;89(5):711–31.
[16] Viatour P, Merville MP, Bours V, Chariot A. Phosphorylation of nf-kappab and ikappab proteins: implications in cancer and inflammation. Trends Biochem Sci 2005;30(1):43–52.
[17] Yu M, Yeh J, Van Waes C. Protein kinase casein kinase 2 mediates inhibitor-kappaB kinase and aberrant nuclear factor-kappaB activation by serum factor(s) in head and neck squamous carcinoma cells. Cancer Res 2006;66(13):6722–31.
[18] Romieu-Mourez R, Landesman-Bollag E, Seldin DC, Sonenshein GE. Protein kinase CK2 promotes aberrant activation of nuclear factor-kappaB, transformed phenotype, and survival of breast cancer cells. Cancer Res 2002;62(22):6770–8.
[19] Brown MS, Diallo OT, Hu M, Ehsanian R, Yang X, Arun P, et al. CK2 modulation of NF-kappaB, TP53, and the malignant phenotype in head and neck cancer by anti-CK2 oligonucleotides *in vitro* or *in vivo* via sub-50-nm nanocapsules. Clin Cancer Res 2010;16(8):2295–307.
[20] Yang L, Liu N, Hu X, Zhang W, Wang T, Li H, et al. CK2 phosphorylates TNFAIP1 to affect its subcellular localization and interaction with PCNA. Mol Biol Rep 2010;37(6):2967–73.
[21] Hu X, Yan F, Wang F, Yang Z, Xiao L, Li L, et al. TNFAIP1 interacts with KCTD10 to promote the degradation of KCTD10 proteins and inhibit the transcriptional activities of NF-kappaB and AP-1. Mol Biol Rep 2012;39(11):9911–9.
[22] Zhao X, Zhao L, Yang H, Li J, Min X, Yang F, et al. Pyruvate kinase M2 interacts with nuclear sterol regulatory element-binding protein 1a and thereby activates lipogenesis and cell proliferation in hepatocellular carcinoma. J Biol Chem 2018;293(17):6623–34.
[23] Wu H, Yang TY, Li Y, Ye WL, Liu F, He XS, et al. TRAF6 promotes hepatocarcinogenesis by interacting with HDAC3 to enhance c-Myc gene expression and protein stability. Hepatology 2019.
[24] Wang Q, Gao G, Zhang T, Yao K, Chen H, Park MH, et al. TRAF1 is critical for regulating the BRAF/MEK/ERK pathway in non-small cell lung carcinogenesis. Cancer Res 2018;78(14):3982–94.
[25] Goeminne L, Gevaert K, Clement L. Experimental design and data-analysis in label-free quantitative LC/MS proteomics: a tutorial with MSqRob. J Proteomics 2018;171:23–36.
[26] Liu J, Zhang C, Zhao Y, Yue X, Wu H, Huang S, et al. Parkin targets HIF-1alpha for ubiquitination and degradation to inhibit breast tumor progression. Nat Commun 2017;8(1):1823.
[27] Mahdi AH, Huo Y, Tan Y, Simhadri S, Vincelli G, Gao J, et al. Evidence of intertissue differences in the dna damage response and the pro-oncogenic role of nf-kappab in mice with disengaged BRCA1-PALB2 interaction. Cancer Res 2018;78(14):3969–81.
[28] Liu X, Li C, Yang Y, Liu X, Li R, Zhang M, et al. Synaptotagmin 7 in twist-related protein 1-mediated epithelial - Mesenchymal transition of non-small cell lung cancer. EBioMedicine 2019;46:42–53.
[29] Yang L, Qiu J, Xiao Y, Hu X, Liu Q, Chen L, et al. AP-2beta inhibits hepatocellular carcinoma invasion and metastasis through slug and snail to suppress epithelial-mesenchymal transition. Theranostics 2018;8(13):3707–21.
[30] Zhang CL, Wang C, Yan WJ, Gao R, Li YH, Zhou XH. Knockdown of TNFAIP1 inhibits growth and induces apoptosis in osteosarcoma cells through inhibition of the nuclear factor-kappaB pathway. Oncol Rep 2014;32(3):1149–55.
[31] Li J, Xu Y, Long XD, Wang W, Jiao HK, Mei Z, et al. Cbx4 governs HIF-1alpha to potentiate angiogenesis of hepatocellular carcinoma by its SUMO E3 ligase activity. Cancer Cell 2014;25(1):118–31.
[32] Guttridge DC, Albanese C, Reuther JY, Pestell RG, Baldwin AJ. NF-kappaB controls cell growth and differentiation through transcriptional regulation of cyclin D1. Mol Cell Biol 1999;19(8):5785–99.
[33] Suboj P, Babykutty S, Valiyaparambil GD, Nair RS, Srinivas P, Gopala S. Aloe emodin inhibits colon cancer cell migration/angiogenesis by downregulating MMP-2/9, RhoB and VEGF via reduced DNA binding activity of NF-kappaB. Eur J Pharm Sci 2012;45(5):581–91.
[34] Sternlicht MD, Werb Z. How matrix metalloproteinases regulate cell behavior. Annu Rev Cell Dev Biol 2001;17:463–516.
[35] Song R, Song H, Liang Y, Yin D, Zhang H, Zheng T, et al. Reciprocal activation between ATPase inhibitory factor 1 and NF-kappaB drives hepatocellular carcinoma angiogenesis and metastasis. Hepatology 2014;60(5):1659–73.
[36] Geyer R, Wee S, Anderson S, Yates J, Wolf DA. BTB/POZ domain proteins are putative substrate adaptors for cullin 3 ubiquitin ligases. Mol Cell 2003;12(3):783–90.
[37] Eddy SF, Guo S, Demicco EG, Romieu-Mourez R, Landesman-Bollag E, Seldin DC, et al. Inducible ikappab kinase/IkappaB kinase epsilon expression is induced by CK2 and promotes aberrant nuclear factor-kappaB activation in breast cancer cells. Cancer Res 2005;65(24):11375–83.
[38] McElhinny JA, Trushin SA, Bren GD, Chester N, Paya CV. Casein kinase II phosphorylates I kappa B alpha at S-283, S-289, S-293, and T-291 and is required for its degradation. Mol Cell Biol 1996;16(3):899–906.
[39] Bird TA, Schooley K, Dower SK, Hagen H, Virca GD. Activation of nuclear transcription factor nf-kappab by interleukin-1 is accompanied by casein kinase II-mediated phosphorylation of the p65 subunit. J Biol Chem 1997;272(51):32606–12.
[40] Zhang M, Gao C, Yang Y, Li G, Dong J, Ai Y, et al. MiR-424 promotes non-small cell lung cancer progression and metastasis through regulating the tumor suppressor gene TNFAIP1. Cell Physiol Biochem 2017;42(1):211–21.
[41] Zhang P, Guo Z, Hu R, He X, Jiao X, Zhu X. Interaction between microRNA-181a and TNFAIP1 regulates pancreatic cancer proliferation and migration. Tumour Biol 2015;36(12):9693–701.
[42] Xing S, Zhang B, Hua R, Tai WC, Zeng Z, Xie B, et al. URG4/URGCP enhances the angiogenic capacity of human hepatocellular carcinoma cells *in vitro* via activation of the NF-kappaB signaling pathway. BMC Cancer 2015;15:368.
[43] Chantome A, Pance A, Gauthier N, Vandroux D, Chenu J, Solary E, et al. Casein kinase II-mediated phosphorylation of NF-kappaB p65 subunit enhances inducible nitric-oxide synthase gene transcription *in vivo*. J Biol Chem 2004;279(23):23953–60.

[44] Chua M, Lee M, Dominguez I. Cancer-type dependent expression of CK2 transcripts. PLoS ONE 2017;12(12):e188854.
[45] Cavin LG, Romieu-Mourez R, Panta GR, Sun J, Factor VM, Thorgeirsson SS, et al. Inhibition of CK2 activity by TGF-beta1 promotes IkappaB-alpha protein stabilization and apoptosis of immortalized hepatocytes. Hepatology 2003;38(6):1540–51.
[46] Yu W, Ding X, Chen F, Liu M, Shen S, Gu X, et al. The phosphorylation of SEPT2 on Ser218 by casein kinase 2 is important to hepatoma carcinoma cell proliferation. Mol Cell Biochem 2009;325(1–2):61–7.
[47] Wu D, Sui C, Meng F, Tian X, Fu L, Li Y, et al. Stable knockdown of protein kinase CK2-alpha (CK2alpha) inhibits migration and invasion and induces inactivation of hedgehog signaling pathway in hepatocellular carcinoma Hep G2 cells. Acta Histochem 2014;116(8):1501–8.
[48] Wu S, Wolf DA. Destruction of RhoA CULtivates actin. Mol Cell 2009;35(6):735–6.
[49] Murakami A, Maekawa M, Kawai K, Nakayama J, Araki N, Semba K, et al. Cullin-3/KCTD10 E3 complex is essential for Rac1 activation through RhoB degradation in human epidermal growth factor receptor 2-positive breast cancer cells. Cancer Sci 2019;110(2):650–61.